Available online freely at www.isisn.org

Bioscience Research

Print ISSN: 1811-9506 Online ISSN: 2218-3973

Journal by Innovative Scientific Information & Services Network

RESEARCH ARTICLE BIOSCIENCE RESEARCH, 2020 17(3): 2331-2357. **OPEN ACCESS**

Evaluation of locally made horizontal penetrometer to measure soil compaction under Egyptian conditions

Meselhy A. A.

Agricultural Mechanization Unit, Soil and Water Conservation Department - Desert Research Center, **Egypt**

***Correspondence: adil_meselhy@yahoo.com** **Received 07-07-2020, Revised: 13-09-2020, Accepted: 23-09-2020 e-Published: 30-09-2020**

Measuring soil penetration resistance is one of the most important measurements that express the soil compaction status. Soil compaction is an important physical limiting factor for the root growth and plant emergence and is one of the major causes for reduced crop yield worldwide, thus determining the type and degree of tillage that suit the soil conditions. The traditional vertical penetrometer is the famous device to measure soil penetration resistance. The data collected by it are not sufficient to characterize the soil compaction status, as there may be a variation in the soil compaction values in one site, which requires taking several measurements to obtain high accuracy in the measurement, which requires a great effort and time. Therefore, the objective of this study was to achieve a more accurate, less effort and faster way to measure soil penetration resistance and generate soil compaction maps for different depth layers of the soil. To do so, a locally made horizontal penetrometer designed and manufactured, which mounted on an agricultural tractor, consisted of a mechanical system and data acquisition system (DAS) tabulate the measured quantities. After that, soil compaction maps could be generated using data collected. The data automatically stratified to determine soil compaction distribution at different layers. The system was successfully tested in field conditions, in Ras-Suder Research Station, South Sinai, in sandy loam soil where, nine levels of device forward speed with tractor were studied (0.5, 1, 1.5, 2, 2.5, 3, 3.5, 4 and 4.5) $km.h^{-1}$ and three levels of measurement depth (20, 30 and 40) cm. The soil penetration resistance measurements of the proposed horizontal penetrometer were compared with the traditional vertical penetrometer at the same measurement locations and soil depths, for calibration the horizontal penetrometer and calculation the correction factor at different speeds and measurement depths where, found that horizontal penetrometer reading was greatly affected by their change. A multiple regression equation calculated to determine the horizontal penetrometer reading correction factor by the speed and measurement depth. So, with this equation, the correction factor of horizontal penetrometer readings calculated by knowing both the speed of movement and measurement depth of the penetrometer. Then maps created to describe soil penetration resistance at various depths. Thus, a complete picture of the soil compaction status available by the least time and effort as well as high accuracy. This allows determining the optimum tillage type that used. The horizontal penetrometer evaluated by studying the effect of forward speed of the device's movement with the tractor on the draft force (kN), fuel consumption rate ($l.h^{-1}$), fuel consumption per unit area ($l.ha^{-1}$) and actual field capacity ($ha.h^{-1}$). The results showed that an increasing percentage in draft force, fuel consumption rate and actual field capacity were about of 197%, 191% and 610%, respectively, with an increasing the forward speed from 0.5 to 4.5 $km.h^{-1}$. The optimum speed of the horizontal penetrometer, which achieved the lowest fuel consumption per unit area ($l.ha^{-1}$), was determined to be about of 3.13 $km.h^{-1}$. It was concluded that the system tested in this study could be used to assess the distribution of compaction at soil different layers, and to create maps that give a visualization of the spatial variation of the compaction distribution in the soil at different depths,

from which it is possible to determine the appropriate type and degree of tillage.

Keywords: critical depth, horizontal penetrometer, penetration resistance, soil compaction, soil mapping,

INTRODUCTION

Soil compaction is one of the main negative factors that limits plant growth and crop yield. Therefore, it is important to determine the soil resistance level and map it for the field to find solutions for the negative effects of the compaction. The tractors, tillage tools and the machine systems, which used in the agricultural production, can cause field traffic. Especially today's machines such as powerful tractors, combine harvesters etc. which are becoming heavier because of their additional attached equipment, have become a reason for high level of soil compaction observed in agricultural fields. Another reason for soil compaction is tillage in non-suitable terms of the soil. In addition to these external effects, natural effects such as excessive rainfall and drought can also be a reason for high levels of soil compaction (Tekin, et al., 2008).

Soil compaction is an important physical limiting factor for the root growth and plant emergence, decreasing crop production worldwide. Soil compaction may significantly debilitate the production capacity of soil by reducing porosity, creating obstacles to air, water, nutrient movements and root penetration (Raper, et al. 2005). In addition, soil compaction reduces rate of leaf appearance and ground cover expansion, shortened canopy cover duration and restricted light interception, which combined to reduce tuber yield (Stalham, et al. 2007). Reductions in grain yield attributable to soil compaction for several climate and crops in a wide range of soils from sands to heavy clays (Bayhan et al. 2002 and Gregory et al. 2007). Moreover, the subsoil becomes a compacted soil layer, which prevents water from infiltrating into deeper layers, resulting in reduced porosity at topsoil and decreased yields (Al-Adawi and Reeder, 1996). Therefore, researchers are interested in focusing on subsoil compaction and the methods of tillage to control the compacted layer (Filipovic et al. 2006 and Keller and Arvidsson, 2006). Soil compaction has long been noted to cause root restrictions and yield reductions in many crops in the world (McConnell et al. 1989; Mullins et al. 1992). Compaction, which increases soil strength and decreases soil aeration, can restrict the growth of plant roots and negatively affect the environment (Hillel, 1980; Soane And Van Ouwerkerk, 1995). In general, (soil cone index, CI) varies greatly with depth in the rooting zone, and is affected by soil properties such as water content, bulk density and particle size distribution (e.g., clay content) (Guerif, 1994). Perumpral, (1987) stated that CI increased with increasing soil density and decreasing soil water content. Elbanna and Witney, (1987) expressed CI at an average tillage depth as a function of clay fraction, cohesive and frictional coefficients, soil water content and soil specific weight. Researches on compaction interference in agricultural productivity are numerous, regarding soil physical properties and root distribution and growth (Cavallini et al., 2010; Secco et al. 2009; Silva et al. 2009; Reichert et al. 2009; Gubiani et al.2013). Soil compaction can also influence agricultural machinery and implement performances, promoting an expansion in potency demand for traction (Drescher et al. 2011; Mentges et al. 2010). To diagnose compaction, penetrometers or penetrographs used, however, requiring considerable time to obtain data as reported by (Adamchuk and Molin, 2006). Certain research areas have been seeking for alternatives to improve soil potential use and consequently increasing crop yields. For instance, crop and soil mapping to aid in applying inputs at variable rates, and sectorial management using precision agriculture tools (Machado, 2013). One of the basic precision agriculture practices is to define soil property spatial variability within a farming area to make decisions that can maximize crop profitability and reduce negative environmental impacts, according to Dhillon et al. (2010).

Soil cone penetrometers used as an indicator of the soil resistance. Previous studies using penetrometers showed that the crop growth is limited if the soil penetration value is greater than 2-3 MPa (300-435 psi) depending on the crop type (Ehlers et al. 1983). According to Horn and Baumgartl, (2000) proper root development in many instances is observed when penetration resistance is under 2 MPa. Soil compaction commonly expressed as penetration resistance (PR) measured by a soil cone penetrometer. A simple penetrometer is a penetration rod having a conical tip with a force sensor, which may be a strain gauge or piezoelectric load cell (Sun et al., 2004). PR defined as the penetration force divided by a standard cone base area during the penetration of the soil with a standard soil cone penetrometer at a constant penetration rate. The standard penetrometer cone has a 30° cone tip

angle and a 2.54 mm base diameter. The penetration rate also standardized as 30 $mm.s^{-1}$. Although there is more than one method to assess soil compaction, the most convenient method for most researchers in field conditions for monitoring and assessing soil compaction has long been using handheld penetrometers. Thus, the accuracy of PR measurements is highly related to the ability to maintain a constant probe speed (ASAE, 1994). Traditionally, penetration resistance measured using a standardized cone penetrometer (ASABE Standards, 2006a). A cone penetrometer consists of a rod with a 30° cone-shaped tip attached to a load-measuring device. While the cone is inserted vertically at a constant rate (3 $cm.s^{-1}$), the insertion force is measured along with the depth of insertion. The ratio of this force to the area of the cone base called the cone index (CI) and represents the soil penetration resistance. The vertically operated cone penetrometer has been traditionally used to assess the soil mechanical resistance within a soil profile. The cone penetrometer measures the force required to insert a cone tip into the soil. Cone index (CI) calculated by dividing this insertion force by the base area of the cone. This point-based measurement method makes it difficult to obtain enough data to represent spatial variability across an agricultural field. The cone penetrometer is not a practical method to determine soil compaction in a large-scale field (Raper et al. 1999). Soil examination techniques in the field have been widely used for many centuries. They used for evaluating the quality of land, for studies of soil genesis, soil compaction, erosion control, and for tillage management. One of the problems in measuring compaction and other soil characteristics is a quick and accurate method of making the measurement. The two major objections to the use of most soil penetrometers are the laborious process of manually pushing the cone into the soil media and recording individual reading obtained at specified intervals (Batey and McKenzie, 2006). Wells et al. (2001) and Wells et al. (2005) mapped the spatial distribution of soil compaction as indicated by cone penetrometer resistance (soil cone index, CI) on multiple fields. From these maps, it was possible to determine the type and degree of tillage the soil needed. They concluded that precision tillage produced increased yield relative to compacted cells receiving no deep tillage in five of six crops studied. Weisbach and Wilde, (1997) used a pull-type horizontal penetrometer to measure penetration force at three different depths simultaneously and they reported that 35% of the study field did not need deep tillage. Penetration resistance measurements usually related to soil moisture content and bulk density. Therefore, researchers developed models to relate soil compaction to dry bulk density and soil moisture content (Dexter, et al. 2007 and Cui, et al.2007). Some studies show that PR randomly varies across the fields (Castrignanò, et al. 2002). In practice, however, collecting enough point data with high accuracy across a whole field, so that geo-referenced soil compaction maps can be produced, requires long time and excessive efforts. Recently, studies focus more on the use of horizontal penetrometers with electronic kits for mapping soil compaction. The soil compaction maps allow researchers and farmers to pin out where exactly the soil compaction occurs (Carrara, et al. 2007). Thus, the farmer can observe how soil compaction varies at different locations and depths across the field. Because direct field measurements of compaction are difficult, soil strength is often used as a surrogate measurement (Canarache, 1991), with the cone penetrometer being the primary measurement device (ASAE Standards, 2003a, 2003b). However, cone penetrometer readings are discrete point measurements, making it difficult to collect enough data to accurately represent within-field variations in soil strength. A soil strength sensor able to obtain measurements at multiple depths continuously while traveling across the field would be much more efficient in detecting compacted zones, and several such prototype sensors have been developed (Glancey et al. 1989; Adamchuk et al. 2001; Andrade et al. 2001; Chukwu and Bowers, 2005). The cone penetrometer is the tool most often used to quantify soil strength in situ (Mulqueen et al. 1977). The index of soil strength measured by a cone penetrometer, cone index (CI), is defined as the force per unit base area required to push the penetrometer through a specified small increment of depth at a standard insertion rate (ASAE, 2005a,b). Cone penetrometer readings require a “stop-and-go” procedure with data collected at discrete locations, making it difficult to collect enough data to accurately map compaction variations within a field.

Additionally, penetrometer data are highly variable even at a single location and require several readings to obtain representative measurements. Even in non-spatial analyses, researchers have often collected hundreds of penetrometer readings to investigate treatment differences (Busscher et al. 1986) and to relate cone index to soil properties such as water content and bulk density (Sojka et al. 2001). The soil cone penetrometer has been traditionally used to assess the soil strength within a soil profile. The cone penetrometer measures the force required insert a cone tip into the soil. Cone index calculated by dividing this insertion force by to base area of the cone. Cone index is an empirical measurement of soil state and measures the net effect of several soil properties (ASAE Standards, 2004b). In order to be able to make constant measurements, efforts have been made to design horizontally operated penetrometers. These are structures consisting of a horizontally oriented penetrating tip attached to a load cell and supported by heavy shanks. The implement can be mounted to the tractor. The results showed that increasing of soil resistance force as the horizontal penetrometer speed increased. (Sun et al. 2006). Soil failure does not occur in the same manner at all the operating depths as it depends on factors such as soil structure and critical depth (Hemmat et al. 2009). In Figure (1), transition from crescent to lateral failure occurs at d/w > 6 (Godwin and O'Dogherty, 2007). Abbas, et al., (2009) mention that the horizontal penetrometer sensor was tested in a field with silty clay loam soil at three depths of 10, 15 and 20cm. The results showed that average horizontal soil mechanical resistance index (HRI) values for both depths of 10 and 15cm were similar due to the brittle failure mode in both cases. However, when the tip was operated below the critical depth of the sensor, the value of HRI at 20cm depth increased three times when compared with 10 or 15cm depth values. This was due to change in failure mode from brittle to compressive mode below the critical depth. There was a significant relationship (R = 0.75) between HRI and vertical penetrometer CI for the 20cm depth, whereas for shallower depths the relation was not significant. It can be concluded that the correlation between measurements obtained with the vertically and horizontally operated penetrometers would be significant as long as both produced the same soil failure mode. For a tip-based sensor, when the tip width is smaller than the shank, the critical depth is dependent on the aspect ratio (working depth/tine width) of the shank and not of the tip. Ultimately, the correlation between measurements obtained with the vertically and horizontally operated penetrometers would be significant as long as the sensing tip of soil horizontal resistance sensor was operated below the critical depth and induced similar failure mode. The plowed soil as a testing medium did not present any variability, but had local effects (soil clods) as compared to soils below the plowed layer. The performance of horizontal penetrometer sensors has generally been evaluated with respect to standard vertical penetrometer. However, such a comparison can be problematic because the failure modes produced by on-the-go sensors and vertically operated penetrometers might be different. By nature, soil mechanical resistance sensors are of soil failure type. Chisel or knife-type (tine-based) sensor acts as a simple rigid tine, whereas a shank (leg) equipped with a horizontal sensing tip (tip-based sensor) acts as a rigid tine with leading tip. The soil ahead of the cone tip of the vertically operated penetrometer is always in the bearing-capacity failure mode, whereas for both tine and tip based sensors, this type of failure would occur only if they operated under the critical depth (Hemmat and Adamchuk, 2008). A horizontal measuring system with multiple sensors was designed and built to measure mechanical impedance of soil at different depths over the entire top 400 mm of the soil profile. The vertical penetrometer data was averaged over 10 cm intervals and compared to the average force measurements from each sensors of measurement system. There was a correlation with $R^2 = 0.77$ (the least correlation coefficient) at 0-100mm depth and

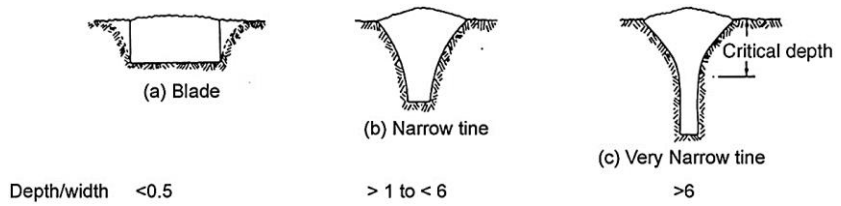

Figure (1): Effect of tool depth/width ratio on patterns of soil failure, (Godwin and O'Dogherty, 2007).

R^2 = 0.83 (the most correlation coefficient) at 300-400mm depth between vertical penetrometer data and horizontal measurement system values. However, due to thickness of shank and soil failures problem occurring in front of the shank, the existing system was not precise. There are still improvements to be made for higher accuracy and reliability of sensing devices. The draft requirement for horizontal penetrometer in different soil types and conditions depended on working depth, working speed, soil type, physical condition and strength properties (Abbaspour-Gilandeh, (2009). Abbas et al., (2012) reported that, the soil failure mode ahead of two horizontally operated penetrometers was investigated and the following results were observed:

1- The critical depth at which the soil failure mode changed from brittle to compressive was at a working depth/shank width ratio of around 6.

2-At shallow depths and above the critical depth, the sensor tip moved through the disturbed soil. Therefore, the failure mode (brittle type) ahead of the sensor tip was different from the mode (compressive type) observed ahead of a vertically operated cone penetrometer.

3-Below the critical depth, the failure mode (compressive type) ahead of the sensor tips had similar soil disturbance patterns as a vertically operated cone penetrometer.

Therefore the objective of this research was to evaluate a locally prototype of horizontal penetrometer able to detect soil penetration resistance at three different layers, as well as collecting data for mapping of soil layers with management purposes. In addition, evaluation the effect of operation speed on horizontal penetrometer performance to obtained optimum speed under study conditions.

MATERIALS AND METHODS

Field-testing:

For the field measurements, the working depths of the horizontal penetrometer were (20, 30 and 40) cm and the forward speeds were (0.5, 1, 1.5, 2, 2.5, 3, 3.5, 4, and 4.5) $km.h^{-1}$ by a proper combination of gear ratio and engine speed. The working depth was set so that the sensing tip of the horizontal penetrometer was located below the critical depth of the penetrometer tine where soil is not already disturbed by the tine (Naderi-Boldaji et al. 2013b). Consequently, there is no effect of the device shank in breaking up the soil in front of it during movement, and this does not affect the reading of a device as shown in Figure (2). In order to make the penetration of the sensor tips into the soil easier, a pit with a depth of 500-600 mm was excavated at the start of each pass, and then the shank with sensors put into the pit. In this way, the sensor tips found their way into the soil without any difficulty. The experiment land was divided into rectangles, each one 5m x 10m, so that the average measure of soil resistance is taken by it. The experiment area was divided into 10 rectangles in width and 8 rectangles in length to form a plot of 80m x 50m with an area of $4000m^2$, as shown in Figure (3). Testing of the sensor was conducted in Ras-suder research station located south of Sinai Governorate on sandy loam soil (latitude: 29° 37' 26'' N, longitude: 32° 42' 43'' E and the elevation from sea surface = 36.2m). A sandy loam is soil containing a high percentage of sand (Coarse sand 12.3% - Fine sand 58.7%), but having enough silt (19.7%) and clay (9.3%) to make it somewhat coherent. The average moisture content, bulk density and penetration resistant (for vertical penetrometer VPS) of soil surface layers (20, 30 and 40) cm were determined as shown in Table (1). The soil had been in a no-tillage after a wheat harvest in May 2019. The field area was approximately 4000 m^2. Two methods were used to measure soil penetration resistance in the field, the horizontal penetrometer system (HPS) and a standard vertical cone penetrometer a Japanese cone index, model (SR-2, DIK-500) as traditional system (VPS) as shown in Figure (4) utilized to examine the data that were collected with the HPS.

Components of the horizontal penetrometer system (HPS):

The horizontal penetrometer system (HPS) is composed of three components: a sensing tip, a shank, and a force transducer as shown in Figure (5). The shank was mounted to a frame, and the frame was attached to a tractor as shown in Figure (6). The shank was designed to provide a method of inserting the force transducer and the soil resistant sensing tips into the soil. The shank was constructed from 20 × 150 mm plate steel, with a total shank length of 700 mm. The shank was designed to be pushed at a perpendicular rake angle to the soil surface. The shank was designed so that the sensor would have a maximum effective measuring depth of 600mm. To limit the formation of a soil wedge in front of the advancing shank, the leading edge of the shank was beveled to form a 30° prismatic wedge similar to the impedance sensing tips. This bevel should eliminate any soil from forming on the front of the shank and maintain consistent force values as the shank pushed through the soil (Gill and Vanden Berg, 1968). The

shank was designed to penetrate vertically into the soil profile with minimum downward force. To facilitate this penetration into the soil profile, the bottom of the shank was cut on a 45° angle and beveled to a 30° prismatic wedge as shown in Figures (7, 8 and 9). A 30mm tall × 50mm deep section was removed from the back of the shank to position the sensing tip flush with the leading edge of the shank. A 15mm hole was drilled through the center of the removed section to allow the impedance tip to pass through the shank unobstructed and connect to the force transducer placed on the back of the shank. A square tube cable protector was welded to the rear of the shank to prevent damage to the force transducer cable. The force transducer chosen for the HPS was a 2.54 kN measurement capacity. Since the base cross-sectional area of the tip of the HPS developed in the present study is 254 mm^2, if the maximum expected soil strength of soil is assumed to be 10 MPa, the maximum force measured at each tip is 10 MPa × 254 mm^2 = 2.54 kN. Sensing tip protruded 30mm in front of the advancing shank. The impedance tip was connected to the force transducer by a 12mm beam, which passed through an oversized hole drilled in the shank as shown in Figure (10). This beam connected from the front to the tip, and the back end connected with a variable electrical resistance so that the movement of the beam back and forward moves the electrical resistance with it, and therefore its value changes, so the current intensity changes in the electrical circuit of each tip. Each electrical circuit of each tip connected to the inlet of the oscilloscope, which measures the electrical current intensity.

Sensor development and calibration:

For conducting this experimental work, a tine with a multi-tips horizontal sensor using replaceable cone tips, was developed to measure the soil penetration resistance at multiple depths. The width of tine was 20 mm. The apex angle of both tips was 30º with the same base area of 254 mm^2 (The diameter of the base of the cone was 18 mm) (ASAE Standard, 2005a). The tips were mounted horizontally on the tine face. The sensing shafts were mounted horizontally on the tines, and their depths were 20, 30 and 40 cm from soil surface. The sensing unit of system as shown in Figure (10) mounted on the backside of each shaft and contact with oscilloscope device to measuring and recording the change of output voltages by change in variable resistance. This change in variable resistance was made by the shaft, which connected between it and the cone. Each sensing unit of the instrumented tine was calibrated in the laboratory by applying known forces and measuring output voltages as shown in Figure (11).

Specifications of oscilloscope device model Hantek 6104BD:

- Analog input channels: Four.
- Material: Aluminum Alloy + Plastic.
- Bandwidth: 100 MHz.
- Oscilloscope Probe Model: PP-150.
- Device Size: Approx. 210 * 125 * 37 mm.
- Sampling Rate: 1GSa/s.
- Portable: PC-Based.
- Bandwidth: 100 MHz.
- Input Sensitivity: 2mV/div to 10V/div.
- Vertical Resolution: 8 bits.

Actual field capacity.

Actual field capacity calculated by using equations mentioned by kepner et al., (1978).

Pulling force.

Pulling force measured by hydraulic dynamometer, which, coupled between the two tractors with the attaching horizontal dynamometer to estimate its draught force. The average of 10 readings of the draught force taken in 10 seconds intervals.

Fuel consumption rate.

Fuel consumption per unit time was determined by measuring the volume of fuel consumed during operation time. It was measured using the fuel meter equipment as shown in Figure (12). The length of line, which marked by the marker tool on the paper sheet represents the fuel consumption. The fuel meter was calibrated prior and the volume of fuel was determined accurately.

Fuel consumption per unit area

Fuel consumption per unit area was determined by using the following equation:

FCA=FCT/AFC, Where: FCA = Fuel consumption per unit area ($l.ha^{-1}$), FCT = Fuel consumption per unit time ($l.h^{-1}$) and AFC = Actual field capacity ($ha.h^{-1}$).

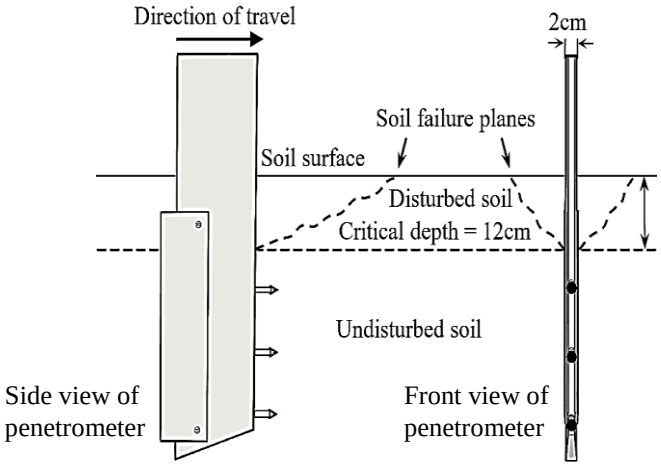

Figure 2: Horizontal penetrometer below the critical depth.

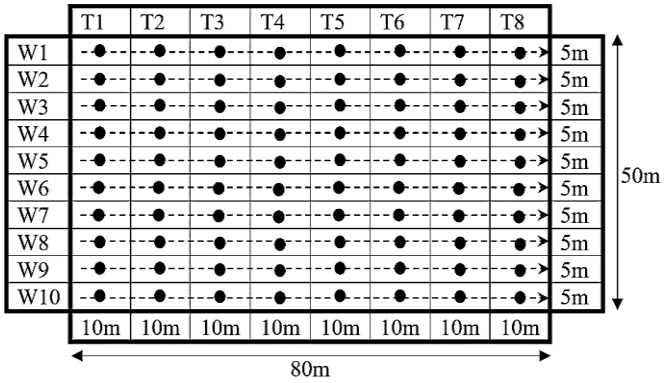

Figure 3: The experiment area 4000 m^2 divided into 10 rectangles in width (80 m) and 8 rectangles in length (50 m). Arrows indicated to movement lines of horizontal penetrometer and points indicated to measure places of vertical penetrometer.

Table 1: Physical properties of experimental soil.

Soil depth (cm)	Average soil penetration resistance of (VPS) (kPa)	Soil bulk density (g.cm^{-3})	Soil moisture content (%)
20	794	1.56	15.38
30	1126	1.71	18.74
40	1592	1.78	20.41

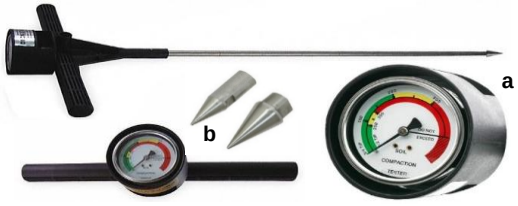

Probe length (In.)	30
Probe Dia. (In.)	0.5
Probe Material	Steel
Pressure Range (PSI)	0 to 500

Figure 4 : Standard vertical cone penetrometer. a: Green testing range (0-200 psi): good growing conditions, yellow testing range (200-300 psi): fair growing conditions and red testing range (300 psi and above): poor growing conditions. b: The small tip used for firm soil and the larger tip.

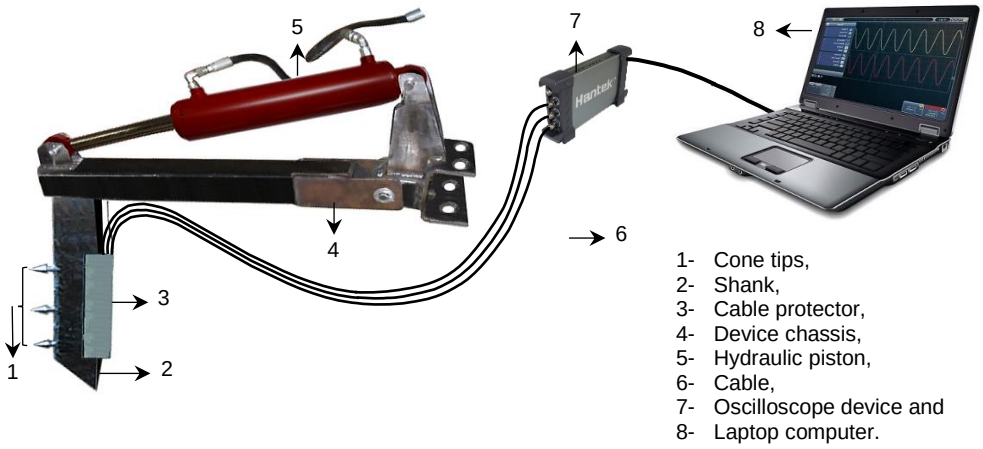

Figure 5 : The horizontal penetrometer system components (HPS).

Figure 6: The horizontal penetrometer attached to a tractor in the field.

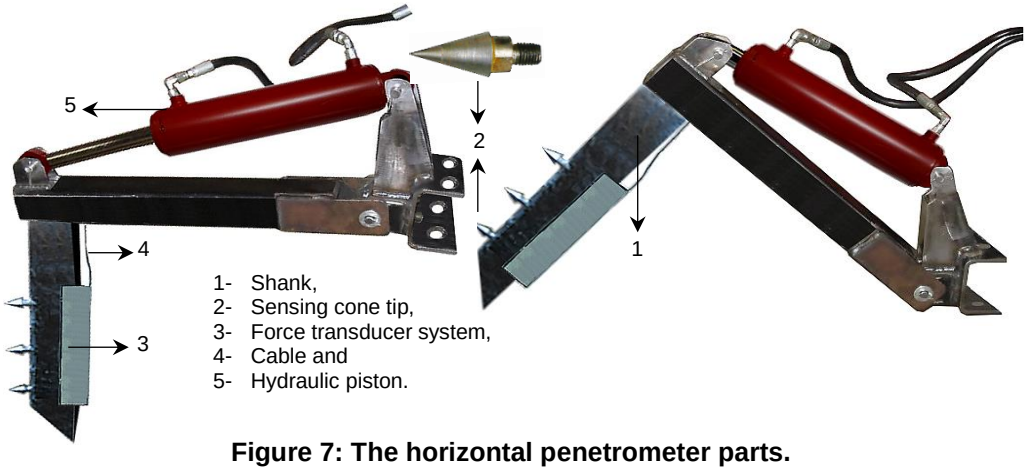

Figure 7: The horizontal penetrometer parts.

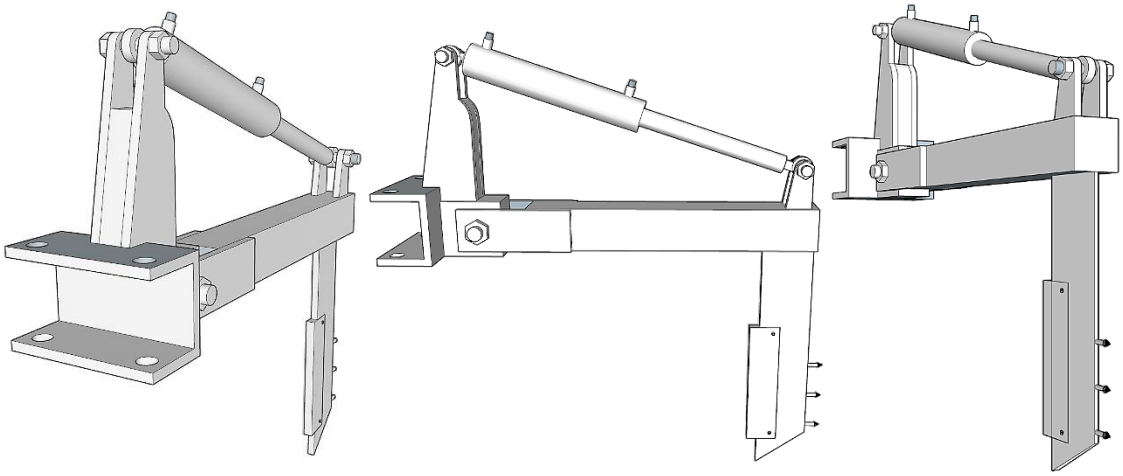

Figure 8 : Illustration shape of the horizontal penetrometer.

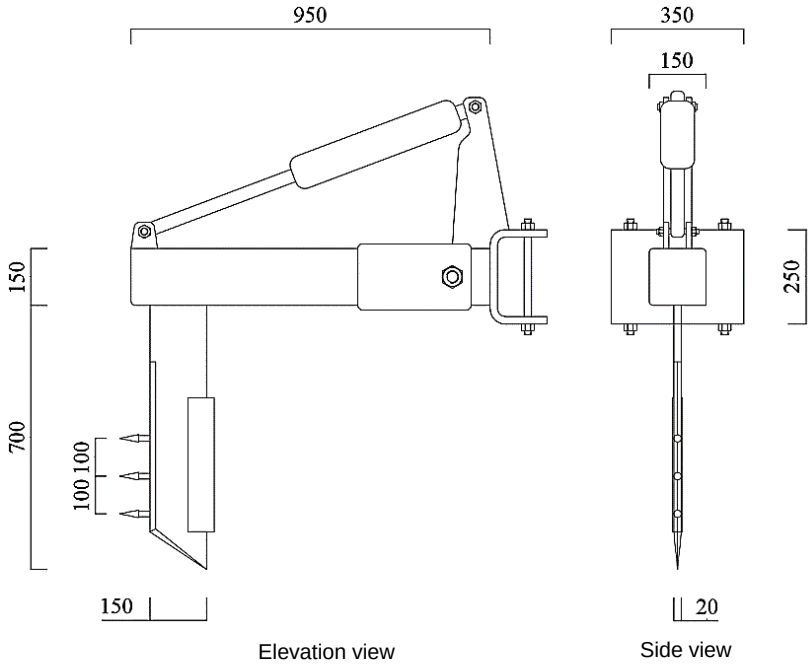

Figure 9 : The horizontal penetrometer.

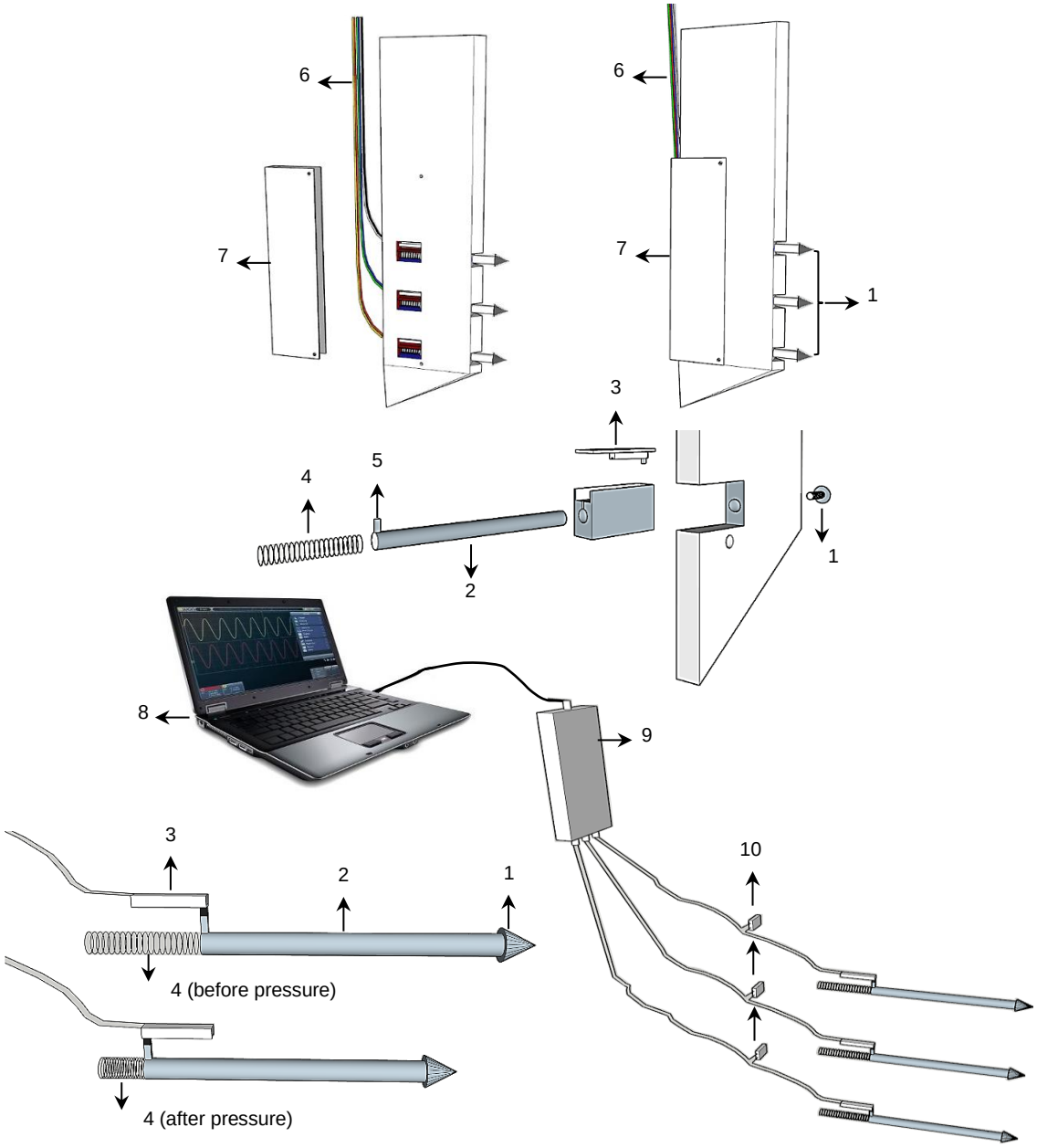

Figure 10 : Mechanism of horizontal penetrometer. The items are (1) cone tip, (2) cone rod, (3) electrical variable resistance, (4), spiral spring, (5) head connect cone rod with electrical variable resistance, (6) cable, (7) cable protector, (8) laptop computer, (9) oscilloscope device and (10) electrical battery.

Figure 11: Calibration for each sensing unit in the laboratory.

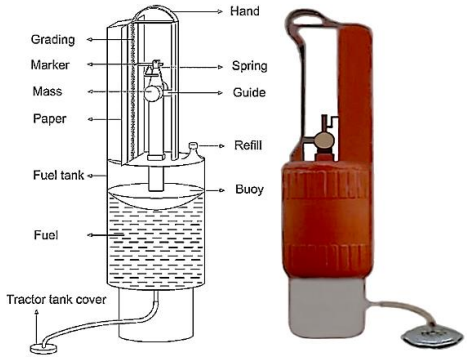

Figure 12: Fuel meter for measuring fuel consumption.

RESULTS AND DISCUSSION

Effect of soil depth and forward speed of horizontal penetrometer on soil penetration resistance:

As shown in Figure (13), the results showed that in general the soil penetration resistance increased with increasing soil depth when using both the vertical and horizontal penetrometer. Where the average percentage increasing in soil penetration resistance was about 100% and 71% when using the vertical and horizontal penetrometers respectively, by increasing the soil depth from 20cm to 40 cm. This result explained because increasing in soil bulk density with increasing depth. The results showed that the forward speed of the horizontal penetrometer had a great effect on its reading. The average percentage of horizontal penetrometer reading increased about 38% when increasing the forward speed from 0.5 $km.h^{-1}$ to 4.5 $km.h^{-1}$, this result was agreement with Sun et al., (2006) showed that the operating speed had significant influence on the soil resistance measurement. The reason for this phenomenon might be due to the air gap around the probe. As the tractor speeded up, the mechanical vibration increased too. Therefore, the influence of the air gap on the measurement results became evident. Results also observed that the horizontal penetrometer reading is always more than the vertical penetrometer reading. In addition, the lowest difference between the reading of horizontal and vertical devices was about 56 kPa at the forward speed of the horizontal penetrometer 0.5 $km.h^{-1}$, while the highest difference was about

520kPa at the speed of 4.5 km.h^{-1}. The reason for this result was the difference in the soil penetration speed between the horizontal and vertical penetrometers. Whereas, the vertical penetrometer penetrates the soil at a constant speed of about 0.11 km.h^{-1}, which is less than the penetration speed of the horizontal penetrometer in this study.

Correction factor:

The horizontal penetrometer reading was corrected by multiplying its reading values by the correction factor as shown in Table (2). The multiple regression equation was obtained to predict the correction factor for the horizontal penetrometer in different soil depths and forward speeds as follows:

$CF = 0.00817\ D - 0.00004\ D^2 - 0.0939\ V + 0.00739\ V^2 + 0.76886$ …… $R^2 = 0.95$

Where: CF = Correction factor, D = Soil depth (cm) and V = Forward speed (km.h^{-1}).

Therefore: Correction values of horizontal penetrometer reading at difference depths and speeds = (horizontal penetrometer reading) x (CF)

The results as shown in Figure (14) explained that the average compatibility ratio between horizontal and vertical penetrometer reading was low and variable with changing in forward speed before the correction process. While, after correcting the readings of horizontal penetrometer by the correction factor as shown in Table (2) the average compatibility ratio between the horizontal and vertical penetrometer reading become high and almost constant about 98%, in spite of the change in the forward speed as shown in Figure (15)

Optimum forward speed for horizontal penetrometer:

In general, the forward speed of the horizontal penetrometer affected on the fuel consumption per unit area l.ha^{-1}, where the fuel consumption decreased when the forward speed increased after that the relationship reversed where the fuel consumption increased when the forward speed increased as shown in Figure (16).

The curve equation of the relationship between fuel consumption per unit area l.ha^{-1} and the forward speed of the horizontal penetrometer was calculated. Then the equation has been differentiated and equal to zero to obtain the forward speed value that achieved the lowest fuel consumption per unit area, which achieved at the speed 3.13 l.ha^{-1} as follows:

$$Y = 0.7075x^2 - 4.4324x + 9.7985$$

$$\frac{dy}{dx} = \frac{d}{dx}(0.7075x^2 - 4.4324x + 9.7985)$$

$$\frac{dy}{dx} = 1.415x - 4.4324$$

Equalize the differential result to zero

$$1.415x - 4.4324 = 0$$

$$1.415x = 4.4324$$

$$x = \frac{4.4324}{1.415} = 3.13\ \mathrm{km.h^{-1}}$$

Performance evaluation of horizontal penetrometer in the field:

The performance of horizontal penetrometer was evaluated by measuring the draft force (kN), fuel consumption rate (l.h^{-1}) and actual field capacity (ha.h^{-1}) at soil depth of 40cm. The Figure (17) showed that the draft force, fuel consumption rate and actual field capacity increased about of 197%, 191%, and 610%, respectively, when the forward speed increasing from 0.5 to 4.5 km.h^{-1}. The results also appeared that fuel consumption per unit area L.ha^{-1} decreased gradually with increasing speed until it reached the lowest value at speed 3.13 km.h^{-1} and then began to gradually increase with increasing speed above 3.13 km.h^{-1}, which indicates that these the optimal value for which the horizontal penetrometer can be used.

Distribution maps of soil penetration resistance:

Figures (18 to 26) showed the distribution maps of soil penetration resistance at different soil depths and forward speeds. The experiment area 4000m^2 divided into 80 rectangular pieces with dimensions of 5 m (width) x 10 m (length). The maps showed the extent of convergence between the corrected horizontal penetrometer readings and the vertical penetrometer readings. Beside the maps, there is a table showed the soil pieces with their penetration resistance values, number of areas with similar values and percentage of these areas respect to the total experiment area at different depths and speeds. These maps can help in making easy the correct and appropriate decision about determine the extent of the soil's need for tillage or not, or determining the degree and suitable tillage depth or decide the type of plow appropriate for the actual soil condition, thus achieving the optimum use of the advantages of the tillage process and avoiding its disadvantages. Which greatly contributes to implement of the precision agriculture system.

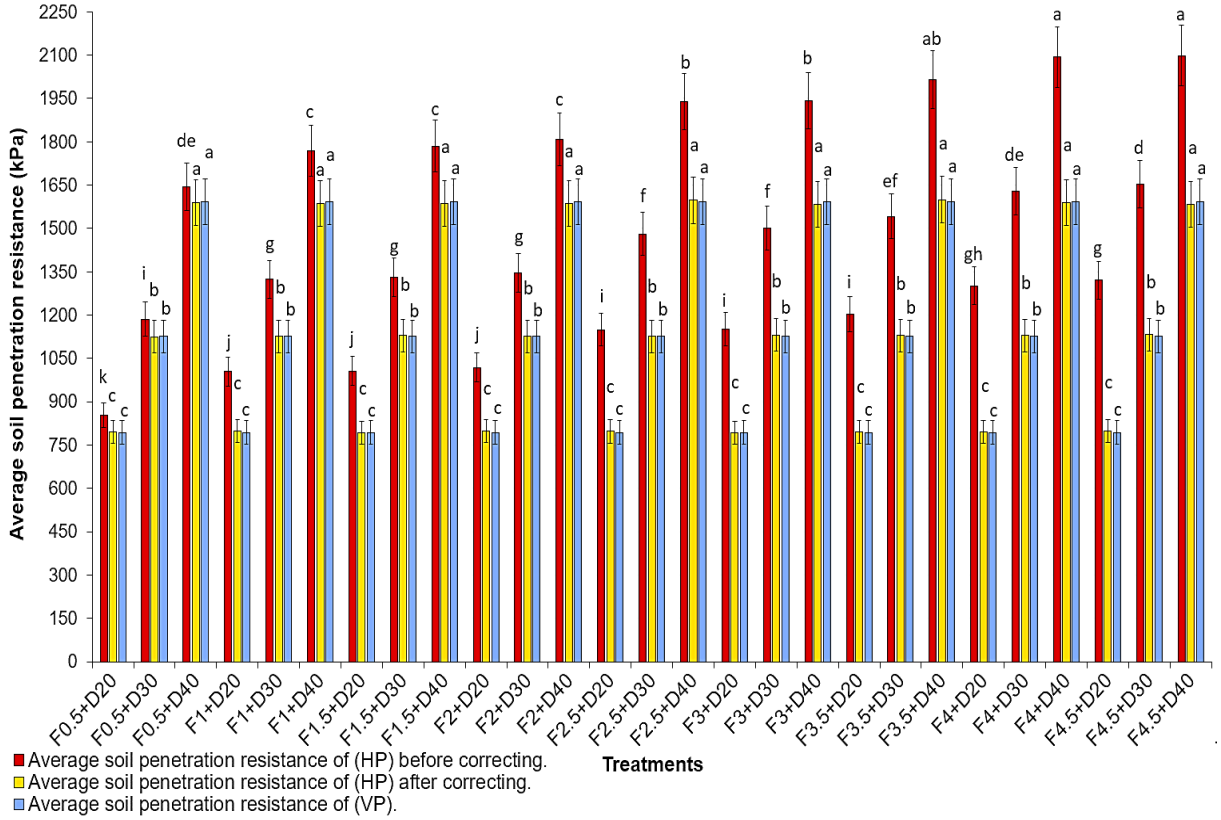

Figure 13: Soil penetration resistance of vertical penetrometer (VP) and horizontal penetrometer (HP) (kPa) before and after correction at different soil depth (D, cm) and forward speed (F, km/h). Values followed by different letters are significantly different at $p < 0.05$ according to the LSD test. Error bars show the standard deviation among the repetitions (n = 3). LSD for: soil penetration resistance of (HP) before correcting = 104, soil penetration resistance of (HP) after correcting = 137 and soil penetration resistance of (VP) = 126.

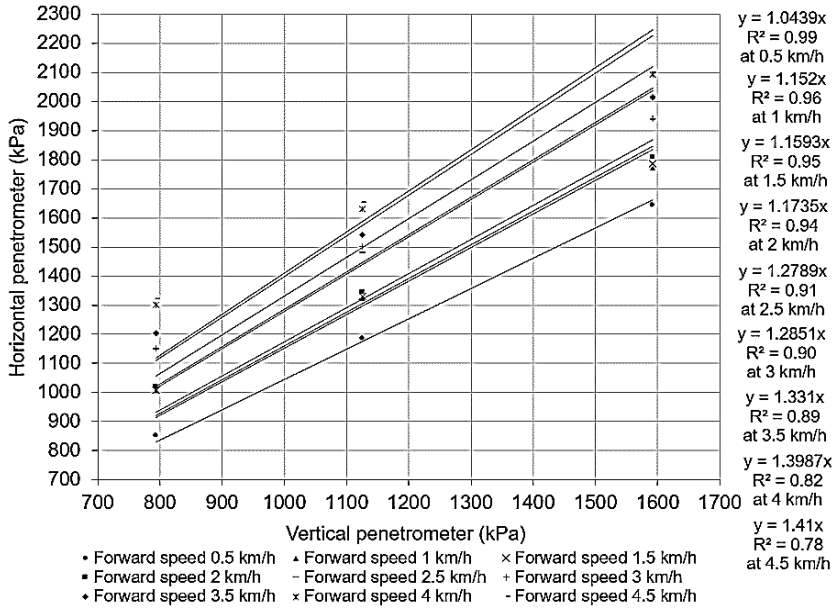

Figure 14: Correlation between soil penetration resistance for horizontal penetrometer and

vertical penetrometer at working depth of 20, 30 and 40 cm before correction values.

Table 2: Correction factor at different forward speed (km.h^{-1}) and soil depth (cm).

Forward speed (km/h)	**0.5**			**1**			**1.5**		
Soil depth (cm)	20	30	40	20	30	40	20	30	40
***Correction factor**	0.93	0.95	0.97	0.79	0.85	0.90	0.79	0.85	0.89
Forward speed (km/h)	2			2.5			3		
Soil depth (cm)	20	30	40	20	30	40	20	30	40
***Correction factor**	0.78	0.84	0.88	0.69	0.76	0.82	0.69	0.75	0.82
Forward speed (km/h)	3.5			4			4.5		
Soil depth (cm)	20	30	40	20	30	40	20	30	40
***Correction factor**	0.66	0.73	0.79	0.61	0.69	0.76	0.60	0.68	0.76

*Correction factor: calculated when soil penetration resistance of vertical penetrometer were 794 kPa, 1126 kPa and 1592 kPa at soil depth 20cm, 30cm an 40cm respectively.

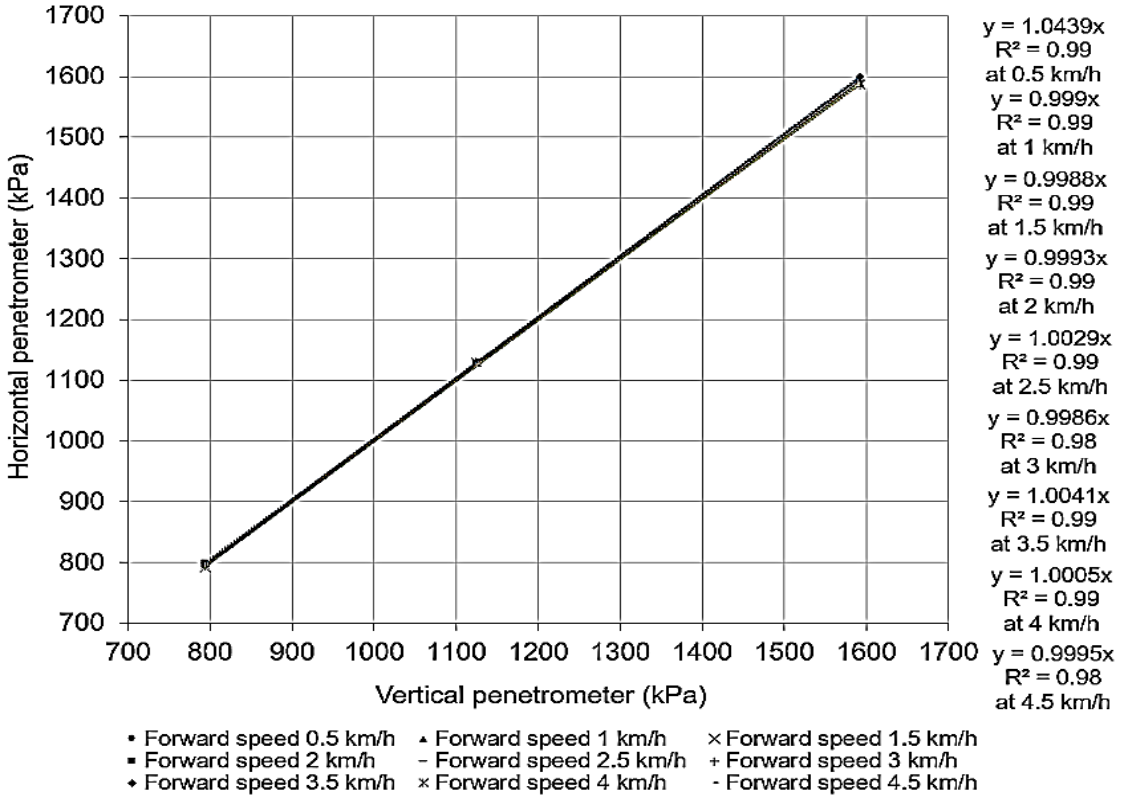

Figure (15): Correlation between soil penetration resistance for horizontal penetrometer and vertical penetrometer at working depth of 20, 30 and 40 cm after correction values.

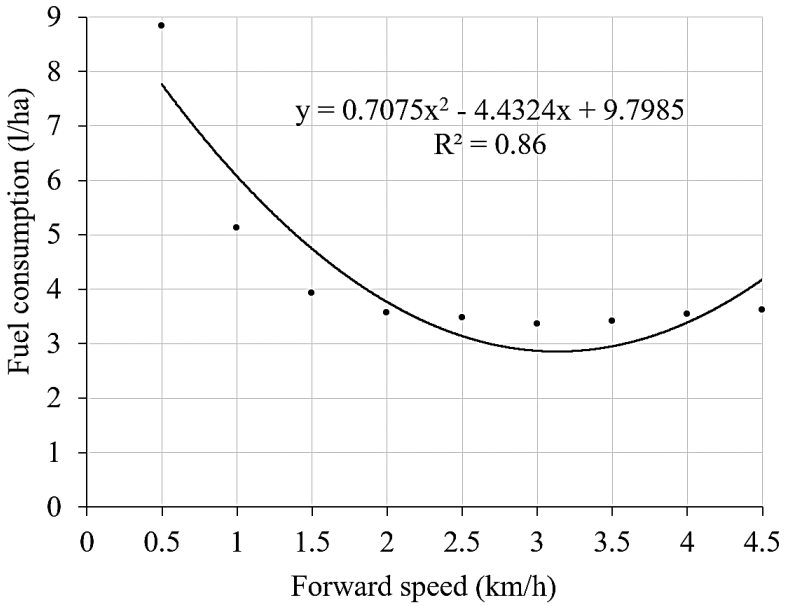

Figure 16: Optimum speed at the lowest fuel consumption.

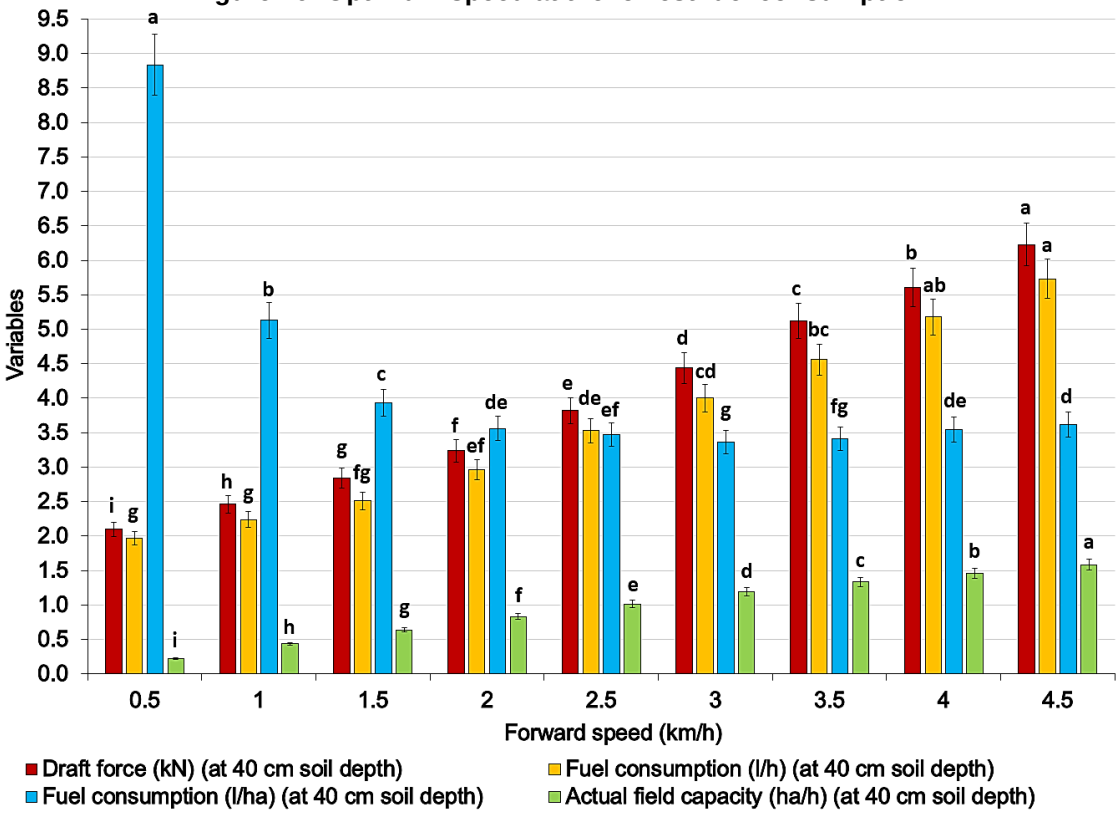

Figure 17: Draft force (kN), fuel consumption (l.h^{-1} and l.ha^{-1}) and actual field capacity (ha.h^{-1}) as affected by forward speed (km.h^{-1}). Values followed by different letters are significantly different at $p < 0.05$ according to the LSD test. Error bars show the standard deviation among the repetitions (n = 3). LSD for: draft force = 0.215, fuel consumption rate = 0.649, fuel consumption per unit area

= 0.092 and actual field capacity = 0.109

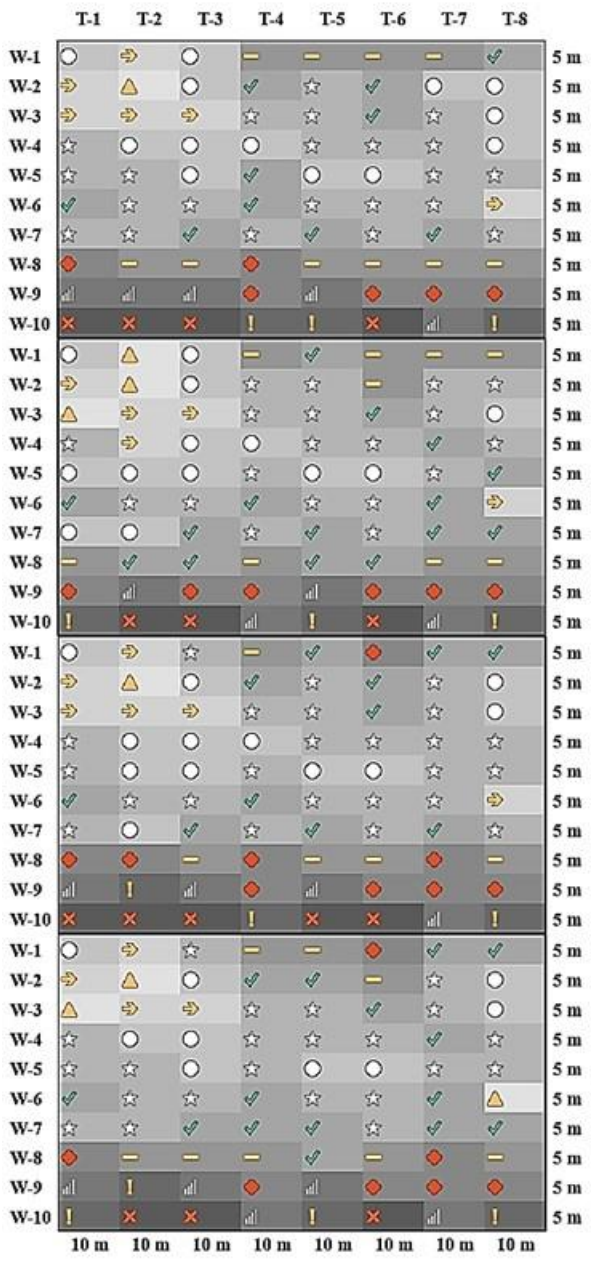

The color	Range of soil penetration resistance (kPa)		Number of area	Area of one piece (m^2)	Area of one color (m^2)	Prcentage of one color (%)
△	732	745	1	50	50	1.25
⇨	746	759	6	50	300	7.5
○	760	773	13	50	650	16.25
☆	774	787	22	50	1100	27.5
✓	788	801	10	50	500	12.5
–	802	815	10	50	500	12.5
◆	816	829	6	50	300	7.5
◢	830	843	5	50	250	6.25
!	844	857	3	50	150	3.75
✖	> 857		4	50	200	5
△	732	745	3	50	150	3.75
⇨	746	759	5	50	250	6.25
○	760	773	13	50	650	16.25
☆	774	787	19	50	950	23.75
✓	788	801	15	50	750	18.75
–	802	815	9	50	450	11.25
◆	816	829	6	50	300	7.5
◢	830	843	4	50	200	5
!	844	857	3	50	150	3.75
✖	> 857		3	50	150	3.75
△	732	745	1	50	50	1.25
⇨	746	759	6	50	300	7.5
○	760	773	12	50	600	15
☆	774	787	24	50	1200	30
✓	788	801	11	50	550	13.75
–	802	815	5	50	250	6.25
◆	816	829	9	50	450	11.25
◢	830	843	4	50	200	5
!	844	857	3	50	150	3.75
✖	> 857		5	50	250	6.25
△	732	745	3	50	150	3.75
⇨	746	759	4	50	200	5
○	760	773	9	50	450	11.25
☆	774	787	22	50	1100	27.5
✓	788	801	15	50	750	18.75
–	802	815	8	50	400	10
◆	816	829	7	50	350	8.75
◢	830	843	5	50	250	6.25
!	844	857	4	50	200	5
✖	> 857		3	50	150	3.75
Total			80	50	4000	100

Figure 18 : Distribution map of soil penetration resistance (kPa) for vertical penetrometer (a) at soil depth 0-20 cm and horizontal penetrometer (b, c, and d) at soil depth 0-20 cm and different forward speeds (0.5, 1 and 1.5 $km.h^{-1}$) respectively.

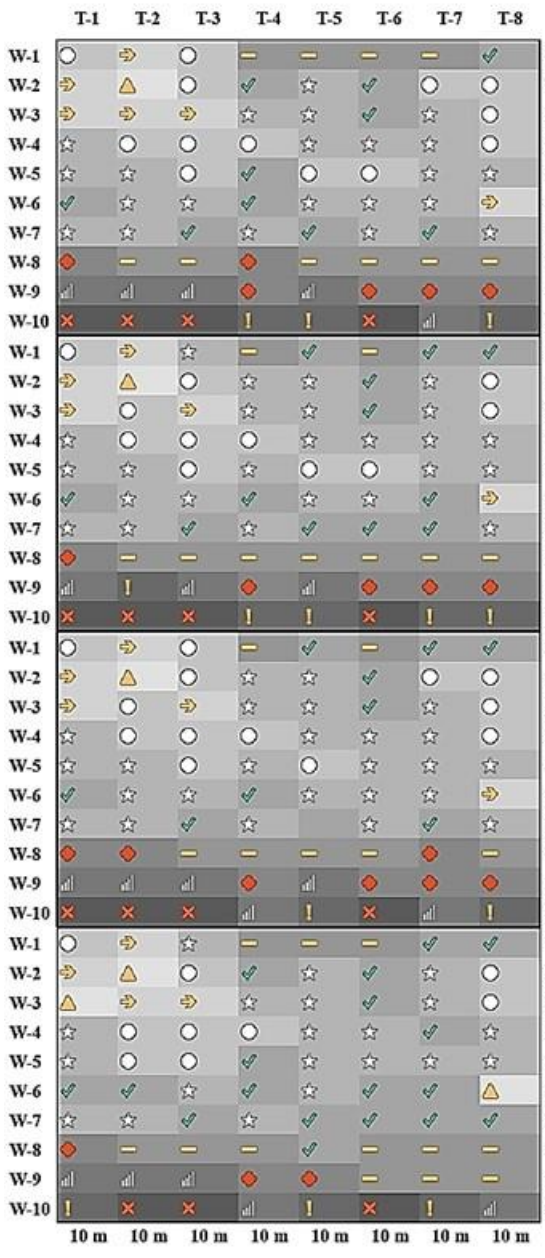

	The color	Range of soil penetration resistance (kPa)		Number of area	Area of one piece (m^2)	Area of one color (m^2)	Prcentage of one color (%)
(a)	△	732	745	1	50	50	1.25
	⇨	746	759	6	50	300	7.5
	○	760	773	13	50	650	16.25
	☆	774	787	22	50	1100	27.5
	✓	788	801	10	50	500	12.5
	–	802	815	10	50	500	12.5
	◆	816	829	6	50	300	7.5
	◢	830	843	5	50	250	6.25
	!	844	857	3	50	150	3.75
	✖	> 857		4	50	200	5
(b)	△	732	745	1	50	50	1.25
	⇨	746	759	5	50	250	6.25
	○	760	773	11	50	550	13.75
	☆	774	787	25	50	1250	31.25
	✓	788	801	12	50	600	15
	–	802	815	9	50	450	11.25
	◆	816	829	5	50	250	6.25
	◢	830	843	3	50	150	3.75
	!	844	857	5	50	250	6.25
	✖	> 857		4	50	200	5
(c)	△	732	745	1	50	50	1.25
	⇨	746	759	5	50	250	6.25
	○	760	773	13	50	650	16.25
	☆	774	787	25	50	1250	31.25
	✓	788	801	10	50	500	12.5
	–	802	815	7	50	350	8.75
	◆	816	829	7	50	350	8.75
	◢	830	843	6	50	300	7.5
	!	844	857	2	50	100	2.5
	✖	> 857		4	50	200	5
(d)	△	732	745	3	50	150	3.75
	⇨	746	759	4	50	200	5
	○	760	773	9	50	450	11.25
	☆	774	787	20	50	1000	25
	✓	788	801	18	50	900	22.5
	–	802	815	12	50	600	15
	◆	816	829	3	50	150	3.75
	◢	830	843	5	50	250	6.25
	!	844	857	3	50	150	3.75
	✖	> 857		3	50	150	3.75
	Total			80	50	4000	100

Figure 19 : Distribution map of soil penetration resistance (kPa) for vertical penetrometer (a) at soil depth 0-20 cm and horizontal penetrometer (b, c, and d) at soil depth 0-20 cm and different forward speeds (2, 2.5 and 3 km.h^{-1}) respectively.

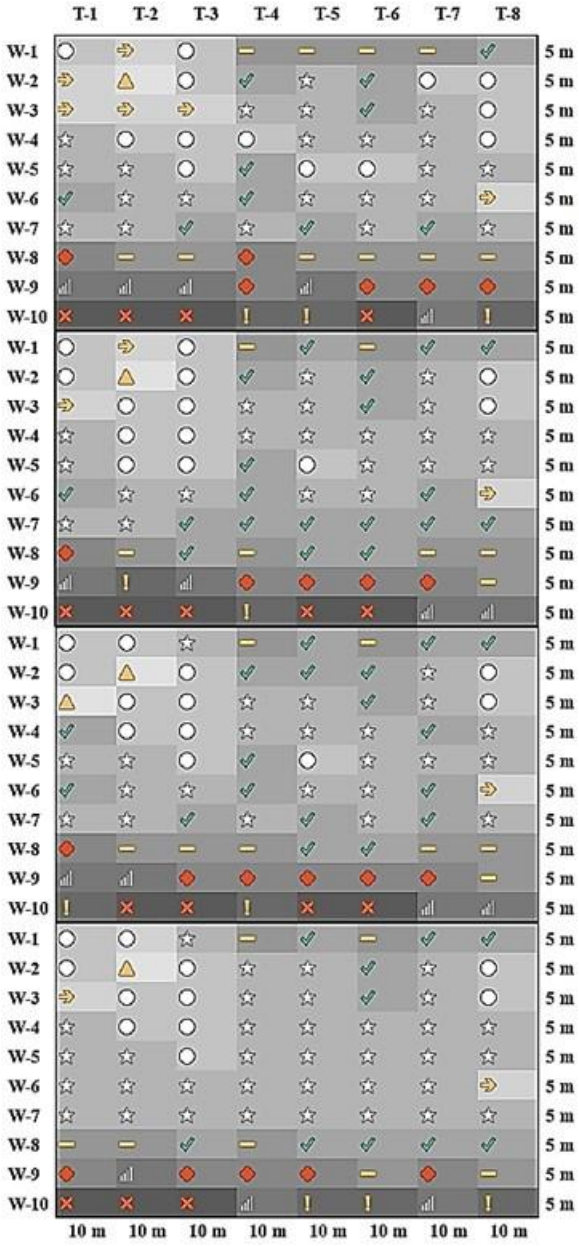

	The color	Range of soil penetration resistance (kPa)		Number of area	Area of one piece (m^2)	Area of one color (m^2)	Prcentage of one color (%)
(a)	△	732	745	1	50	50	1.25
	⇨	746	759	6	50	300	7.5
	○	760	773	13	50	650	16.25
	☆	774	787	22	50	1100	27.5
	✓	788	801	10	50	500	12.5
	–	802	815	10	50	500	12.5
	◆	816	829	6	50	300	7.5
	◢	830	843	5	50	250	6.25
	!	844	857	3	50	150	3.75
	✖	> 857		4	50	200	5
(b)	△	732	745	1	50	50	1.25
	⇨	746	759	3	50	150	3.75
	○	760	773	13	50	650	16.25
	☆	774	787	21	50	1050	26.25
	✓	788	801	19	50	950	23.75
	–	802	815	7	50	350	8.75
	◆	816	829	5	50	250	6.25
	◢	830	843	4	50	200	5
	!	844	857	2	50	100	2.5
	✖	> 857		5	50	250	6.25
(c)	△	732	745	2	50	100	2.5
	⇨	746	759	1	50	50	1.25
	○	760	773	12	50	600	15
	☆	774	787	23	50	1150	28.75
	✓	788	801	18	50	900	22.5
	–	802	815	8	50	400	10
	◆	816	829	6	50	300	7.5
	◢	830	843	4	50	200	5
	!	844	857	2	50	100	2.5
	✖	> 857		4	50	200	5
(d)	△	732	745	1	50	50	1.25
	⇨	746	759	3	50	150	3.75
	○	760	773	10	50	500	12.5
	☆	774	787	35	50	1750	43.75
	✓	788	801	10	50	500	12.5
	–	802	815	7	50	350	8.75
	◆	816	829	5	50	250	6.25
	◢	830	843	3	50	150	3.75
	!	844	857	3	50	150	3.75
	✖	> 857		3	50	150	3.75
	Total			80	50	4000	100

Figure 20: Distribution map of soil penetration resistance (kPa) for vertical penetrometer (a) at soil depth 0-20 cm and horizontal penetrometer (b, c, and d) at soil depth 0-20 cm and different forward speeds (3.5, 4 and 4.5 $km.h^{-1}$) respectively.

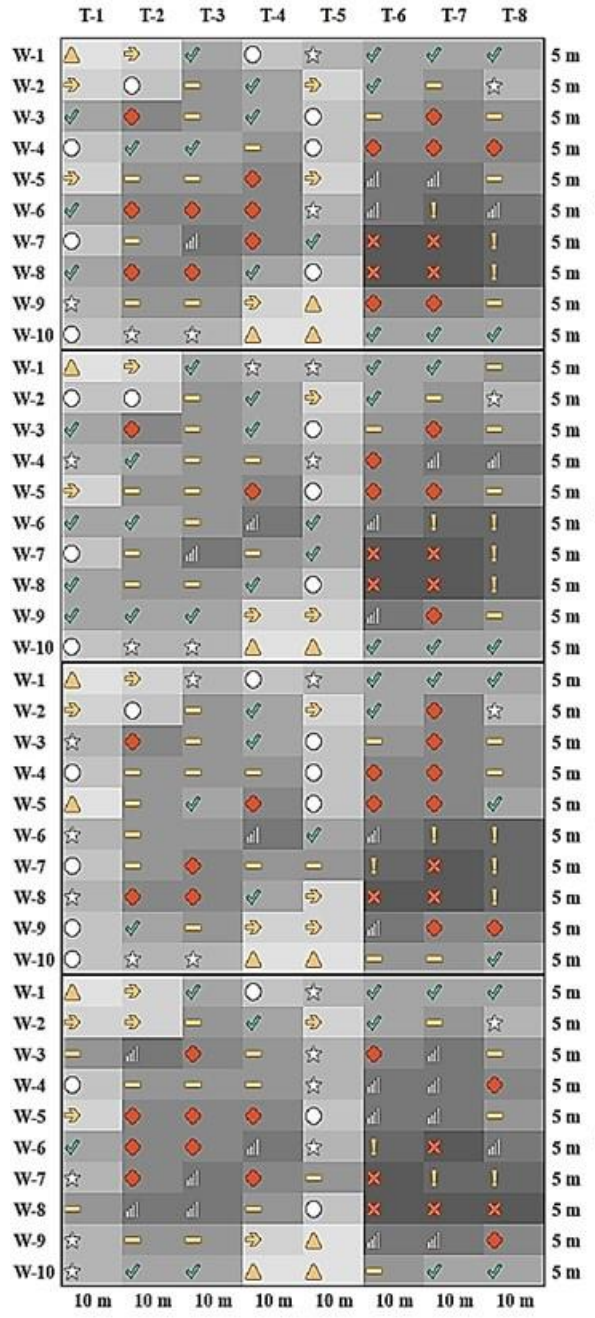

The color	Range of soil penetration resistance (kPa)		Number of area	Area of one piece (m^2)	Area of one color (m^2)	Prcentage of one color (%)
(a)	1068	1079	4	50	200	5
	1080	1091	6	50	300	7.5
	1092	1103	8	50	400	10
	1104	1115	6	50	300	7.5
	1116	1127	17	50	850	21.25
	1128	1139	13	50	650	16.25
	1140	1151	14	50	700	17.5
	1152	1163	5	50	250	6.25
	1164	1175	3	50	150	3.75
	> 1175		4	50	200	5
(b)	1068	1079	3	50	150	3.75
	1080	1091	5	50	250	6.25
	1092	1103	7	50	350	8.75
	1104	1115	7	50	350	8.75
	1116	1127	20	50	1000	25
	1128	1139	17	50	850	21.25
	1140	1151	7	50	350	8.75
	1152	1163	6	50	300	7.5
	1164	1175	4	50	200	5
	> 1175		4	50	200	5
(c)	1068	1079	4	50	200	5
	1080	1091	6	50	300	7.5
	1092	1103	9	50	450	11.25
	1104	1115	8	50	400	10
	1116	1127	12	50	600	15
	1128	1139	17	50	850	21.25
	1140	1151	13	50	650	16.25
	1152	1163	3	50	150	3.75
	1164	1175	5	50	250	6.25
	> 1175		3	50	150	3.75
(d)	1068	1079	4	50	200	5
	1080	1091	6	50	300	7.5
	1092	1103	4	50	200	5
	1104	1115	8	50	400	10
	1116	1127	11	50	550	13.75
	1128	1139	15	50	750	18.75
	1140	1151	11	50	550	13.75
	1152	1163	13	50	650	16.25
	1164	1175	3	50	150	3.75
	> 1175		5	50	250	6.25
	Total		80	50	4000	100

Figure 21 : Distribution map of soil penetration resistance (kPa) for vertical penetrometer (a) at soil depth 20-30 cm and horizontal penetrometer (b, c, and d) at soil depth 20-30 cm and different forward speeds (0.5, 1 and 1.5 $km.h^{-1}$) respectively.

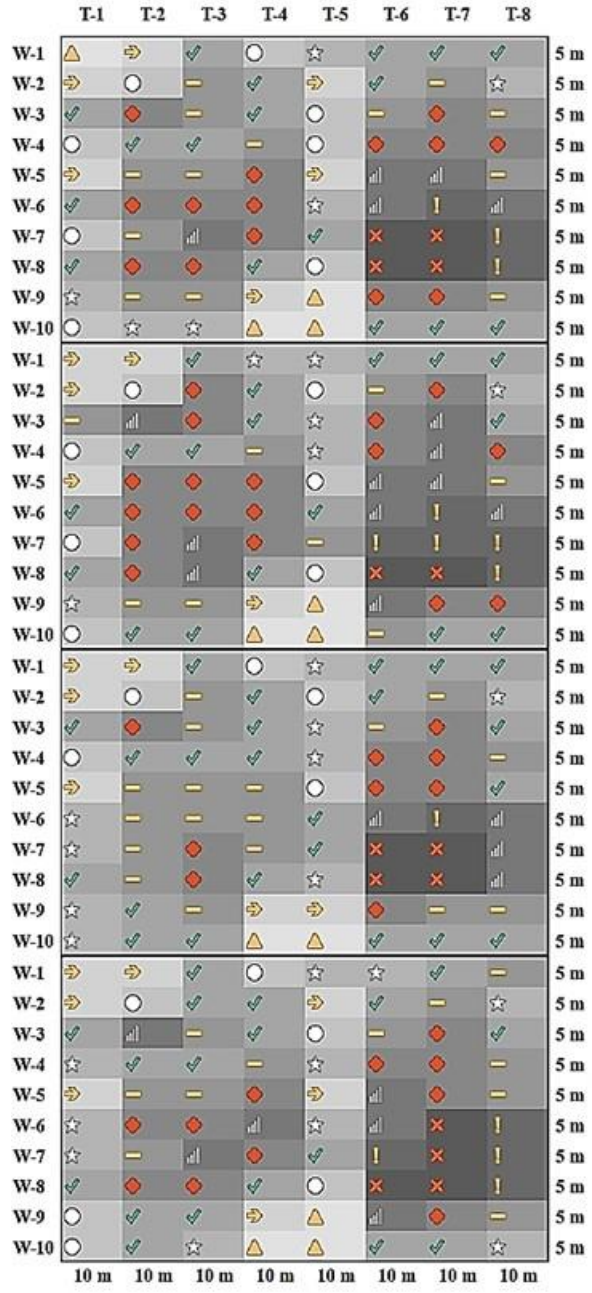

	The color	Range of soil penetration resistance (kPa)		Number of area	Area of one piece (m^2)	Area of one color (m^2)	Prcentage of one color (%)
(a)		1068	1079	4	50	200	5
		1080	1091	6	50	300	7.5
		1092	1103	8	50	400	10
		1104	1115	6	50	300	7.5
		1116	1127	17	50	850	21.25
		1128	1139	13	50	650	16.25
		1140	1151	14	50	700	17.5
		1152	1163	5	50	250	6.25
		1164	1175	3	50	150	3.75
		> 1175		4	50	200	5
(b)		1068	1079	3	50	150	3.75
		1080	1091	5	50	250	6.25
		1092	1103	7	50	350	8.75
		1104	1115	6	50	300	7.5
		1116	1127	17	50	850	21.25
		1128	1139	8	50	400	10
		1140	1151	17	50	850	21.25
		1152	1163	10	50	500	12.5
		1164	1175	5	50	250	6.25
		> 1175		2	50	100	2.5
(c)		1068	1079	2	50	100	2.5
		1080	1091	6	50	300	7.5
		1092	1103	5	50	250	6.25
		1104	1115	9	50	450	11.25
		1116	1127	23	50	1150	28.75
		1128	1139	17	50	850	21.25
		1140	1151	9	50	450	11.25
		1152	1163	4	50	200	5
		1164	1175	1	50	50	1.25
		> 1175		4	50	200	5
(d)		1068	1079	3	50	150	3.75
		1080	1091	7	50	350	8.75
		1092	1103	6	50	300	7.5
		1104	1115	10	50	500	12.5
		1116	1127	18	50	900	22.5
		1128	1139	11	50	550	13.75
		1140	1151	11	50	550	13.75
		1152	1163	6	50	300	7.5
		1164	1175	4	50	200	5
		> 1175		4	50	200	5
		Total		80	50	4000	100

Figure 22 : Distribution map of soil penetration resistance (kPa) for vertical penetrometer (a) at soil depth 20-30 cm and horizontal penetrometer (b, c, and d) at soil depth 20-30 cm and different forward speeds (2, 2.5 and 3 km.h^{-1}) respectively.

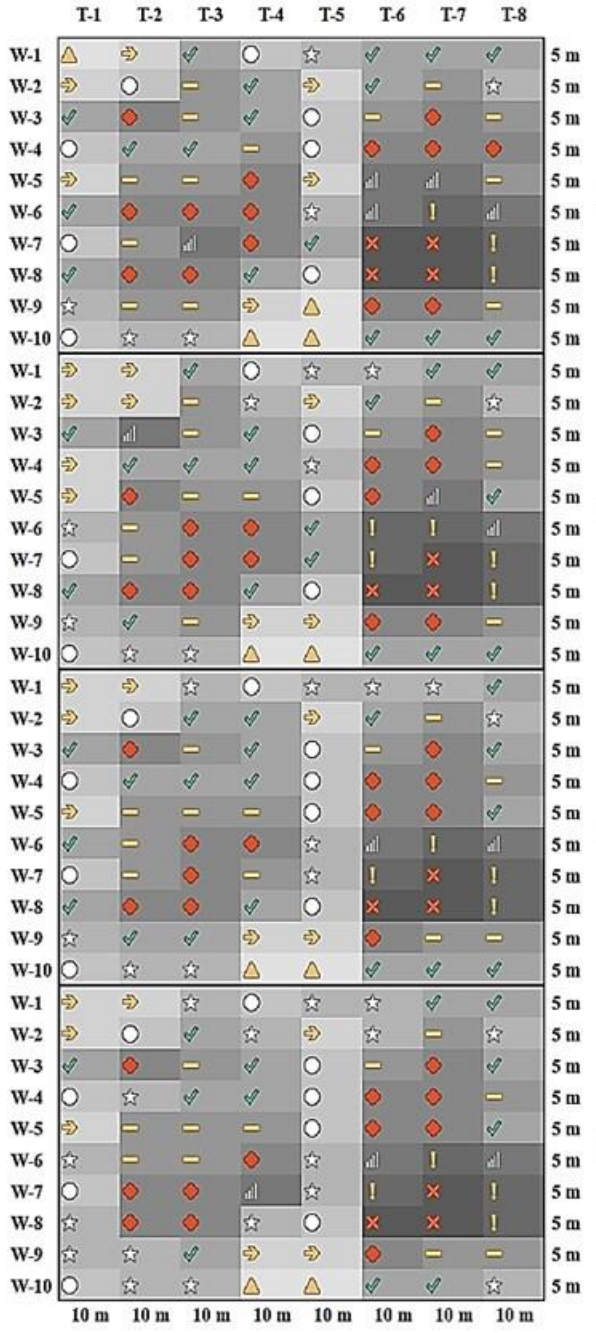

	The color	Range of soil penetration resistance (kPa)		Number of area	Area of one piece (m^2)	Area of one color (m^2)	Prcentage of one color (%)
(a)		1068	1079	4	50	200	5
		1080	1091	6	50	300	7.5
		1092	1103	8	50	400	10
		1104	1115	6	50	300	7.5
		1116	1127	17	50	850	21.25
		1128	1139	13	50	650	16.25
		1140	1151	14	50	700	17.5
		1152	1163	5	50	250	6.25
		1164	1175	3	50	150	3.75
		> 1175		4	50	200	5
(b)		1068	1079	2	50	100	2.5
		1080	1091	9	50	450	11.25
		1092	1103	6	50	300	7.5
		1104	1115	9	50	450	11.25
		1116	1127	18	50	900	22.5
		1128	1139	12	50	600	15
		1140	1151	13	50	650	16.25
		1152	1163	3	50	150	3.75
		1164	1175	5	50	250	6.25
		> 1175		3	50	150	3.75
(c)		1068	1079	2	50	100	2.5
		1080	1091	7	50	350	8.75
		1092	1103	9	50	450	11.25
		1104	1115	10	50	500	12.5
		1116	1127	19	50	950	23.75
		1128	1139	12	50	600	15
		1140	1151	12	50	600	15
		1152	1163	2	50	100	2.5
		1164	1175	4	50	200	5
		> 1175		3	50	150	3.75
(d)		1068	1079	2	50	100	2.5
		1080	1091	7	50	350	8.75
		1092	1103	9	50	450	11.25
		1104	1115	17	50	850	21.25
		1116	1127	12	50	600	15
		1128	1139	11	50	550	13.75
		1140	1151	12	50	600	15
		1152	1163	3	50	150	3.75
		1164	1175	4	50	200	5
		> 1175		3	50	150	3.75
		Total		80	50	4000	100

Figure 23 : Distribution map of soil penetration resistance (kPa) for vertical penetrometer (a) at soil depth 20-30 cm and horizontal penetrometer (b, c, and d) at soil depth 20-30 cm and different forward speeds (3.5, 4 and 4.5 km.h^{-1}) respectively.

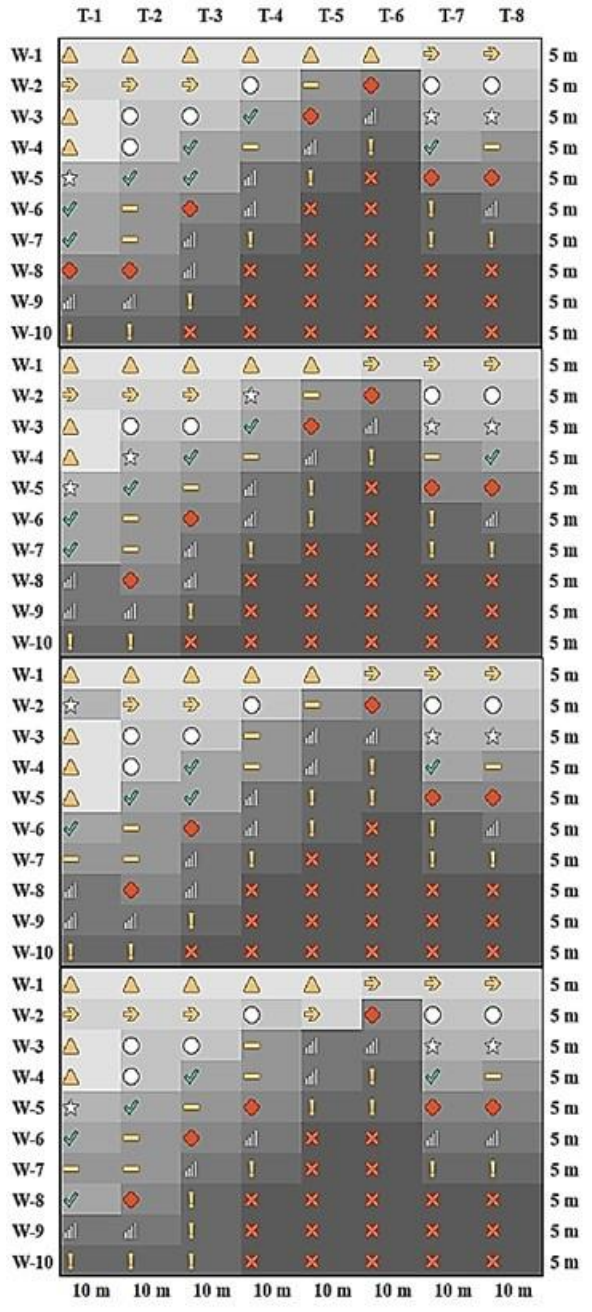

The color	Range of soil penetration resistance (kPa)		Number of area	Area of one piece (m^2)	Area of one color (m^2)	Prcentage of one color (%)
	1311	1356	8	50	400	10
	1357	1402	5	50	250	6.25
	1403	1448	6	50	300	7.5
	1449	1494	3	50	150	3.75
	1495	1540	7	50	350	8.75
	1541	1586	5	50	250	6.25
	1587	1632	7	50	350	8.75
	1633	1678	9	50	450	11.25
	1679	1724	9	50	450	11.25
	> 1724		21	50	1050	26.25
	1311	1356	7	50	350	8.75
	1357	1402	6	50	300	7.5
	1403	1448	4	50	200	5
	1449	1494	5	50	250	6.25
	1495	1540	6	50	300	7.5
	1541	1586	6	50	300	7.5
	1587	1632	6	50	300	7.5
	1633	1678	10	50	500	12.5
	1679	1724	10	50	500	12.5
	> 1724		20	50	1000	25
	1311	1356	8	50	400	10
	1357	1402	5	50	250	6.25
	1403	1448	6	50	300	7.5
	1449	1494	3	50	150	3.75
	1495	1540	5	50	250	6.25
	1541	1586	7	50	350	8.75
	1587	1632	5	50	250	6.25
	1633	1678	11	50	550	13.75
	1679	1724	11	50	550	13.75
	> 1724		19	50	950	23.75
	1311	1356	7	50	350	8.75
	1357	1402	7	50	350	8.75
	1403	1448	6	50	300	7.5
	1449	1494	3	50	150	3.75
	1495	1540	5	50	250	6.25
	1541	1586	7	50	350	8.75
	1587	1632	6	50	300	7.5
	1633	1678	9	50	450	11.25
	1679	1724	11	50	550	13.75
	> 1724		19	50	950	23.75
	Total		80	50	4000	100

Figure 24 : Distribution map of soil penetration resistance (kPa) for vertical penetrometer (a) at soil depth 30-40 cm and horizontal penetrometer (b, c, and d) at soil depth 30-40 cm and different forward speeds (0.5, 1 and 1.5 $km.h^{-1}$) respectively.

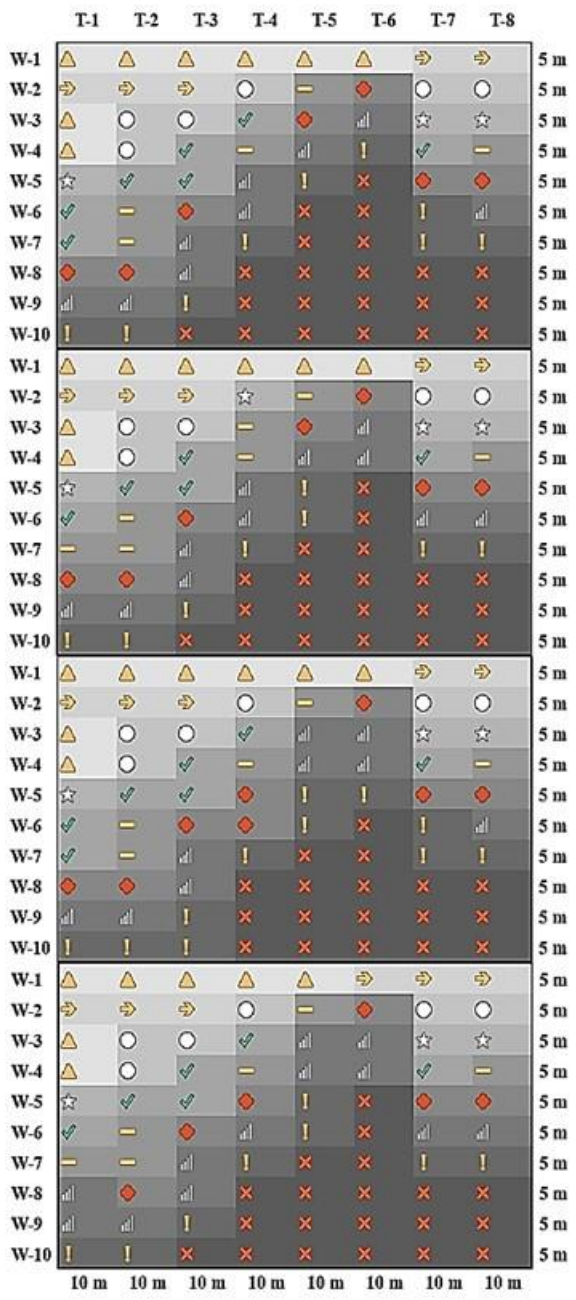

The color	Range of soil penetration resistance (kPa)		Number of area	Area of one piece (m^2)	Area of one color (m^2)	Prcentage of one color (%)
(a)	1311	1356	8	50	400	10
	1357	1402	5	50	250	6.25
	1403	1448	6	50	300	7.5
	1449	1494	3	50	150	3.75
	1495	1540	7	50	350	8.75
	1541	1586	5	50	250	6.25
	1587	1632	7	50	350	8.75
	1633	1678	9	50	450	11.25
	1679	1724	9	50	450	11.25
	> 1724		21	50	1050	26.25
(b)	1311	1356	8	50	400	10
	1357	1402	5	50	250	6.25
	1403	1448	5	50	250	6.25
	1449	1494	4	50	200	5
	1495	1540	5	50	250	6.25
	1541	1586	7	50	350	8.75
	1587	1632	7	50	350	8.75
	1633	1678	11	50	550	13.75
	1679	1724	8	50	400	10
	> 1724		20	50	1000	25
(c)	1311	1356	8	50	400	10
	1357	1402	5	50	250	6.25
	1403	1448	6	50	300	7.5
	1449	1494	3	50	150	3.75
	1495	1540	7	50	350	8.75
	1541	1586	5	50	250	6.25
	1587	1632	8	50	400	10
	1633	1678	9	50	450	11.25
	1679	1724	11	50	550	13.75
	> 1724		18	50	900	22.5
(d)	1311	1356	7	50	350	8.75
	1357	1402	6	50	300	7.5
	1403	1448	6	50	300	7.5
	1449	1494	3	50	150	3.75
	1495	1540	6	50	300	7.5
	1541	1586	6	50	300	7.5
	1587	1632	6	50	300	7.5
	1633	1678	12	50	600	15
	1679	1724	8	50	400	10
	> 1724		20	50	1000	25
	Total		80	50	4000	100

Figure 25 : Distribution map of soil penetration resistance (kPa) for vertical penetrometer (a) at soil depth 30-40 cm and horizontal penetrometer (b, c, and d) at soil depth 30-40 cm and different forward speeds (2, 2.5 and 3 $km.h^{-1}$) respectively.

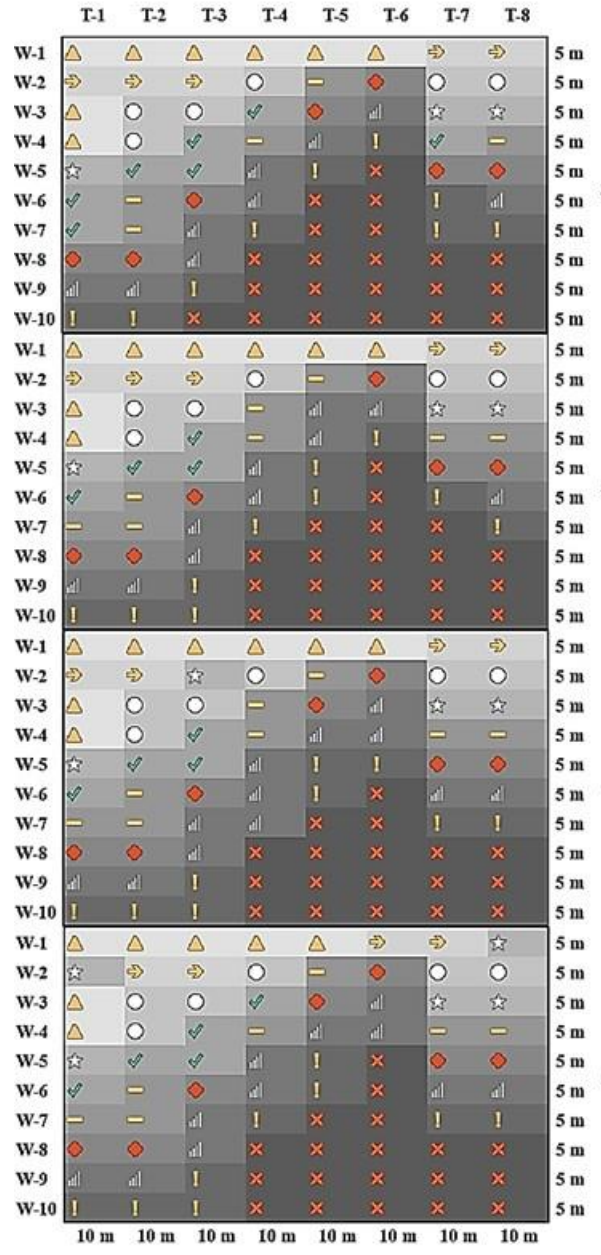

	The color	Range of soil penetration resistance (kPa)		Number of area	Area of one piece (m^2)	Area of one color (m^2)	Prcentage of one color (%)
(a)		1311	1356	8	50	400	10
		1357	1402	5	50	250	6.25
		1403	1448	6	50	300	7.5
		1449	1494	3	50	150	3.75
		1495	1540	7	50	350	8.75
		1541	1586	5	50	250	6.25
		1587	1632	7	50	350	8.75
		1633	1678	9	50	450	11.25
		1679	1724	9	50	450	11.25
		> 1724		21	50	1050	26.25
(b)		1311	1356	8	50	400	10
		1357	1402	5	50	250	6.25
		1403	1448	6	50	300	7.5
		1449	1494	3	50	150	3.75
		1495	1540	4	50	200	5
		1541	1586	8	50	400	10
		1587	1632	6	50	300	7.5
		1633	1678	10	50	500	12.5
		1679	1724	10	50	500	12.5
		> 1724		20	50	1000	25
(c)		1311	1356	8	50	400	10
		1357	1402	4	50	200	5
		1403	1448	6	50	300	7.5
		1449	1494	4	50	200	5
		1495	1540	4	50	200	5
		1541	1586	8	50	400	10
		1587	1632	7	50	350	8.75
		1633	1678	12	50	600	15
		1679	1724	9	50	450	11.25
		> 1724		18	50	900	22.5
(d)		1311	1356	7	50	350	8.75
		1357	1402	4	50	200	5
		1403	1448	6	50	300	7.5
		1449	1494	5	50	250	6.25
		1495	1540	5	50	250	6.25
		1541	1586	7	50	350	8.75
		1587	1632	7	50	350	8.75
		1633	1678	11	50	550	13.75
		1679	1724	9	50	450	11.25
		> 1724		19	50	950	23.75
		Total		80	50	4000	100

Figure 26 : Distribution map of soil penetration resistance (kPa) for vertical penetrometer (a) at soil depth 30-40 cm and horizontal penetrometer (b, c, and d) at soil depth 30-40 cm and different forward speeds (3.5, 4 and 4.5 km.h^{-1}) respectively.

CONCLUSION

In this paper, the horizontal penetrometer was designed to provide a method of rapid determination of soil compaction and its mapping has been discussed. The followings could be concluded as a result of this study:

The horizontal penetrometer mounted on the tractor increased the speed of data collection and hence increased the field efficiency significantly compared to hand-held penetrometers (vertical penetrometer).

From the study, it can be observed that one of the most crucial factors during the data collection

by horizontal penetrometer is speed progress. So that the correction factor was determined to correct the horizontal penetrometer and calculating the multiple regression equation to predict correction factor at different soil depth and forward speed.

The optimum forward speed 3.13 km.h^{-1} was determined for prototype of horizontal penetrometer, which achieved the lowest fuel consumption l.ha^{-1}.

Preliminary evaluation of the horizontal penetrometer indicates that this tool has the potential of measuring soil compaction below critical depth about of 150 mm in this study.

The horizontal penetrometer needs to be evaluated over a wider range of soil conditions and soil types to completely assess the ability of this tool as a general soil compaction-measuring device.

Future studies on this system shall focus on mapping problem areas (locations suffering from compaction with penetration resistance > 2 MPa) and could be used to determine which areas need to tillage and at any depth.

REFERENCES

Abbas H., K. Azar and S. Vahab, (2012). Soil failure mode in front of a multiple-tip horizontally operated penetrometer. Turk J Agric. For 36: 476-485.

Abbas Hemmat, A. Khorsandy, A. A. Masoumi and V. I. Adamchuk, (2009). Influence of failure mode induced by a horizontally operated single-tip penetrometer on measured soil resistance. Soil and Tillage Research 105(1):49-54.

Abbaspour-Gilandeh Y., (2009). On-the-go soil mechanical strength measurement at different soil depths. J. Food Agric. Environ., 7 (3-4), 696-699.

Adamchuk, V. I. and J. P. Molin, (2006). Hastes instrumentadas para mensuração da resistência mecânica do solo. Engenharia Agrícola, Jaboticabal, v. 26, n.1, p.161-169. Disponível em: http:www.sbea.org.br. Acesso em: 4 jan. 2014.

Adamchuk, V. I., M. T. Morgan, and H. Sumali. (2001). Application of a strain gauge array to estimate soil mechanical impedance on-the-go. Trans. ASAE 44(6): 1377-1383.

Al-Adawi, S. S. and R. C. Reeder, (1996). Compaction and subsoiling effects on corn and soybean yields and soil physical properties. Transactions of the ASAE, 39, 1641-1649.

Andrade, P., U. Rosa, S. K. Upadhyaya, B. M. Jenkins, J. Aguera, and M. Josiah. (2001). Soil profile force measurements using an instrumented tine. ASAE Paper No. 011060. St. Joseph, Mich.: ASAE.

ASABE Standards, (2006a). S313.3: Soil cone penetrometer. St. Joseph, Mich.: ASABE.

ASAE Standards, (2003b). EP542: Procedures for using and reporting data obtained with the soil cone penetrometer. St. Joseph, Mich.: ASAE.

ASAE Standards. (2003a). S313.3: Soil cone penetrometer. St. Joseph, Mich.: ASAE.

ASAE Standards. 50th ed. (2004b.) S313.3: Soil cone penetrometer. St. Joseph, Mich.: ASAE.

ASAE, (1994). Soil cone penetrometer. In: ASAE S313.2, Standards engineering practices data.

ASAE, (2005a). Soil Cone Penetrometer. ASAE Standard S313.3, ASAE, St. Joseph, MI.

ASAE, (2005b). Procedures for Using and Reporting Data Obtained with the Soil Cone Penetrometer. ASAE Standard EP542, ASAE, St. Joseph, MI.

Batey, T. D. and C. McKenzie, (2006). Soil compaction: identification directly in the field. Soil Use and Management, 22, 123-131.

Bayhan, Y., B. Kayisoglu and E. Gonulol, (2002). Effect of soil compaction on sunflower growth. Soil & Tillage Research, 68, 31-38.

Busscher, W. J., R. E. Sojka, C. W. Doty, (1986). Residual effects of tillage on coastal plain soil strength. Soil Sci. 141 (2), 144-148.

Canarache, A. (1991). Factors and indices regarding excessive compactness of agricultural soils. Soil and Tillage Res. 19(2-3): 145-164.

Carrara, M., A. Castrignanò, A. Comparetti, P. Febo, and S. Orlando, (2007). Mapping of penetrometer resistance in relation to tractor traffic using multivariate geostatistics. Geoderma, 142, 294-307.

Castrignanò, A., M., Maiorana, F. Fornaro and N. Lopez, (2002). 3D spatial variability of soil

strength and its change over time in a durum wheat field in Southern Italy. Soil & Tillage Research, 65, 95-108.

Cavallini, M. C., M., Andreotti, L. L., Oliveira, C. M. Pariz, and M. P. Carvalho, (2010). Relações entre produtividade de Brachiaria brizantha e atributos físicos de um Latossolo do cerrado. Revista Brasileira de Ciência do Solo, Viçosa, MG, v. 34, n.1, p.1007-1015.

Chukwu, E., and C. G. Bowers, (2005). Instantaneous multiple-depth soil mechanical impedance sensing from a moving vehicle. Trans. ASAE 48(3): 885-894.

Cui, K., P. Défossez and G. Richard, (2007). A new approach for modeling vertical stress distribution at the soil/tyre interface to predict the compaction of cultivated soils by using the PLAXIS code. Soil & Tillage Research 2007, 95, 277–287.

Dexter A. R., E. A. Czyź and O. P. Gate, (2007). A method for prediction of soil penetration resistance. Soil & Tillage Res., 93, 412-419.

Dhillon, R. S., V. I. Adamchuk, K. H. Holland and C. H. Hempleman, (2010). Development of an integrated on-the-go sensing system for soil properties. St Joseph: ASABE. 7 p.

Drescher, M. S., F. L. F Eltz, J. E. Denardin and A. Faganello, (2011). Persistência do efeito de intervenções mecânicas para a descompactação de solos sob plantio direto. Revista Brasileira de Ciência do Solo, Viçosa, MG, v.35, p.713-1722.

Ehlers W., V. Popke, F. Hesse and W. Bohm, (1983). Penetration resistance and root growth of oats in tilled and untilled loam soil. Soil and Tillage Research 3: 261-275.

Elbanna, E. B., B. D. Witney, (1987). Cone penetration resistance equation as a function of the clay ratio, soil moisture content and specific weight. J. Terramech. 24(1), 41-56.

Filipovic, D., S. Husnjak, S., Kosutic and Z. Gospodaric, (2006). Effects of tillage systems on compaction and crop yield of Albic Luvisol in Croatia. Journal of Terramechanics, 43, 177-189.

Gill, W. R., and G. E. Vanden Berg. (1968). Soil Dynamics in Tillage and Traction. Agricultural Handbook No. 316. Auburn, Ala.: USDA.

Glancey, J. L., S. K. Upadhyaya, W. J Chancellor, and J. W. Rumsey, (1996). Prediction of Implement draft using an instrumented analog tillage tool. Soil and Tillage Research, 37(1): 47-65.

Glancey, J. L., S. K. Upadhyaya, W. J. Chancellor, and J. W. Rumsey, (1989). An instrumented chisel for the study of soil-till. dynamics. Soil and Tillage Res. 14(1): 1-24.

Godwin, R. J. and M. J. O'Dogherty, (2007). Integrated soil tillage force prediction models. J. Terramech. 44(1), 3-14.

Gregory, A. S., C. W. Watts, W. R. Whalley, H. L. Kuan, B. S. Griffiths and P. D. Halleth, (2007). Whitmore, A.P. Physical resilience of soil to field compaction and the interactions with plant growth and microbial community structure. European Journal of Soil Science, 58, 1221-1232.

Gubiani, P. I., J. M. Reichert and D. J. Reinert, (2013). Indicadores hídrico-mecânicos de compactação do solo e crescimento de plantas. Revista Brasileira de Ciência do Solo, Viçosa, MG, v.37, p. 1-10.

Guerif, J., (1994). Effects of compaction on soil strength parameters. In: Soane, B.D., Van Ouwerkerk, C. (Eds.), Soil Compaction in Crop Production, 9. Elsevier, Amsterdam, pp. 191-214.

Hemmat, A. and V. I. Adamchuk, (2008). Sensor systems for measuring spatial variation in soil compaction: review and analysis. Comput. Electron. Agric. 63, 89-103.

Hemmat, A., A. Khorsandy, A. A. Masoumi and V. I. Adamchuk, (2009). Influence of failure mode induced by a horizontally operated single-tip penetrometer on measured soil resistance. Soil Tillage Res. 105, 49-54.

Hillel, D. (1980). Applications of Soil Physics. New York, N.Y.: Academic Press.

Horn, R., and T. Baumgartl, (2000). Dynamic properties of soils. In Handbook of Soil Science, A19-A51. M. E. Sumner, ed. Boca Raton, Fla.: CRC Press.

Keller, T. and J. Arvidsson, (2006). Prevention of traffic-induced subsoil compaction in Sweden: Experiencing from wheeling experiments. Archives of Agronomy and Soil Science, 52, 207-222.

Kepner, R. A., R. Bainer and E. L. Barger, (1978). Principles of Farm Machinery. Ch 5, the AVI Publishing Company.

Machado, T. M., (2013). Hastes instrumentadas com controle automatizado do escarificador atuando em profundidades variáveis. 2013. 96 f. Tese (Doutorado em Agronomia) - Faculdade de Ciências Agronômicas, Universidade Estadual Paulista, Botucatu, 2013.

Mcconnell, J. S., B. S. Frizzell, and M. H. Wilkerson, (1989). Effects of soil compaction and subsoil tillage of two alfisols on the growth

and yield of cotton. J. Prod. Agr. 2(2): 140-146.

Mentges, M. I., J. M. Reichert, D. P. Rosa, D. A. Vieira, V. T. Rosa and D. J. Reinert, (2010). Propriedades físico-hidricas do solo e demanda energética de haste escarificadora em Argissolo compactado. Pesquisa Agropecuária Brasileira, Brasília, v. 45, n. 3, p. 315-321.

Mullins, G. L., D. W. Reeves, C. H. Burmester, and H. H. Bryant, (1992). Effect of subsoiling and the deep placement of K on root growth and soil water depletion by cotton. In Proc. Beltwide Cotton Production Research Conf., 1134-1138. Nashville, Tenn.: National Cotton Council.

Mulqueen, J., J. V. Stafford, D. W. Tanner, (1977). Evaluating penetrometers for measuring soil strength. J. Terramech. 14(3), 137-151.

Naderi-Boldaji, M., R. Alimardani, A. Hemmat, A. Sharifi, A. Keyhani, M.Z. Tekeste and T. Keller, (2013b). 3D finite element simulation of a single-tip horizontal penetrometer-soil interaction: Part I: development of the model and evaluation of the model parameters. Soil Tillage Res.134, 153-162.

Perumpral, J. V., (1987). Cone penetrometer applications - aareview. Trans. ASAE 30 (4), 939-943.

Raper, R. L., (2005). Agricultural traffic impacts on soil. Journal of Terramechanics, 42, 259-280.

Raper, R. L., B. H. Washington, and J. D. Jarrell, (1999). A tractor-mounted multiple-probe soil cone penetrometer. Applied Eng. in Agric. 15(4): 287-290.

Reichert, J. M. L. E. A. S. Suzuki, D. J. Reinert, R. Horn and I. Hakansson, (2009). Reference bulk density and critical degree of compactness for no till crop production in subtropical highly weathered soils. Soil and Tillage Research, Amsterdam, v. 102, p. 242-254.

Secco, D., D. J. Reinert, J. M. Reichert and V. R. Silva, (2009). da. Atributos físicos e rendimento de grãos de trigo, soja e milho em dois Latossolos compactados e escarificados. Ciência Rural, Santa Maria, v. 39, p. 58-64.

Silva, V. R., J. M. reichert, D. J. Reinert and E. C. Bortoluzzi, (2009). Soil water dynamics related to the degree of compaction of two Brazilian oxisols under no tillage. Revista Brasileira de Ciência do Solo, Viçosa, MG, v. 33, p. 1097-1104.

Soane, B. D., and C. Van Ouwerkerk, (1995). Implications of soil compaction in crop production for the quality of the environment. Soil and Tillage Res. 35(1-2): 5-22.

Sojka, R. E., W. J. Busscher, G. A. Lehrsch, (2001). In situ strength, bulk density, and water content relationships of a Durinodic Xeric Haplocalcip soil. Soil Sci. 166(8), 520-529.

Stalham, M. A. E. J. Allen, A. B. Rosenfeld and F. X. Herry, (2007). Effects of soil compaction in potato (Solanum tuberosum) crops. Journal of Agricultural Science, 145, 295-312.

Sun Y., D. Ma, P. Schulze Lammers, O. Schmittmann and M. Rose (2006). On-the-go measurement of soil water content and mechanical resistance by a combined horizontal penetrometer. Soil & Tillage Research 86(2):209-217.

Sun, Y. R., P. S. Lammers and D. K. Ma, (2004). Evaluation of a combined penetrometer for simultaneous measurement of penetration resistance and soil water content. Journal of Plant Nutrition and Soil Scie., 167, 745-751.

Tekin, E., B. Kul and R. Okursoy, (2008). Sensing and 3D mapping of soil compaction. Sensors, 8, 3447-3459.

Weissbach, M., and T. Wilde, (1997). The horizontal penetrograph: Big-scale mapping device for soil compaction. In Proc. 3rd International Conference on Soil Dynamics, 244-250. Tiberias, Israel.

Wells L. G., T. S. Stombaugh, S. A. Shearer, (2001). Application and Assessment of Precision Deep Tillage. ASAE Meeting Paper No. 011032. St. Joseph, Michigan, USA.

Wells L. G., T. S. Stombaugh, S. A. Shearer, (2005). Crop yield response to precision deep tillage. Transactions of the ASAE 48(3): 895-901.